
Foundations of Bayesian Learning from Synthetic Data

Harrison Wilde

Department of Statistics
University of Warwick

Jack Jewson

Barcelona GSE
Universitat Pompeu Fabra

Sebastian Vollmer

Department of Statistics,
Mathematics Institute
University of Warwick

Chris Holmes

Department of Statistics
University of Oxford;
The Alan Turing Institute

Abstract

There is significant growth and interest in the use of synthetic data as an enabler for machine learning in environments where the release of real data is restricted due to privacy or availability constraints. Despite a large number of methods for synthetic data generation, there are comparatively few results on the statistical properties of models learnt on synthetic data, and fewer still for situations where a researcher wishes to augment real data with another party’s synthesised data. We use a Bayesian paradigm to characterise the updating of model parameters when learning in these settings, demonstrating that caution should be taken when applying conventional learning algorithms without appropriate consideration of the synthetic data generating process and learning task. Recent results from general Bayesian updating support a novel and robust approach to Bayesian synthetic-learning founded on decision theory that outperforms standard approaches across repeated experiments on supervised learning and inference problems.

1 Introduction

Privacy enhancing technologies comprise an area of rapid growth (The Royal Society, 2019). An important aspect of this field concerns the release of privatised versions of data for learning. Simply *anonymising* data is not sufficient to guarantee individual privacy (e.g. Rocher et al., 2019). Instead, we refer to the large body of work on Differential Privacy (DP) (Dwork et al., 2006) defining bounds on the probability that an adversary may identify whether a particular observation is present in a dataset in the situation where they have access to all other observations in the dataset. DP’s formulation is context-dependent across the literature;

we amalgamate definitions regarding adjacent datasets by Dwork et al. (2014); Dwork and Lei (2009) below:

Definition 1 ((ϵ, δ)-differential privacy) A randomised function or algorithm \mathcal{K} is said to be (ϵ, δ)-differentially private if for all pairs of **adjacent, equally-sized** datasets D and D' that differ in one observation and all $S \subseteq \text{Range}(\mathcal{K})$,

$$\Pr[\mathcal{K}(D) \in S] \leq e^\epsilon \times \Pr[\mathcal{K}(D') \in S] + \delta \quad (1)$$

The current state of the art privatises Generative Adversarial Networks (GANs) (Goodfellow et al., 2014) through adjustments to their learning processes such that their outputs fulfil a DP guarantee specified at the point of training (Jordon et al., 2018; Xie et al., 2018).

Despite these contributions, there is a fundamental knowledge gap surrounding how, from a statistical perspective, one should learn from privatised synthetic data. Progress has been made for simple exponential family and regression models (Bernstein and Sheldon, 2018, 2019). However, the uses of such ‘simple’ models for modern ML problems are limited.

In this paper we ask what does it mean to learn from synthetic data? And how can we improve upon our inferences and predictions given that we acknowledge the privatised synthetic nature of the data? In doing so we adopt the *M-OPEN* world viewpoint (Bernardo and Smith, 2001) associated with model misspecification. We acknowledge that correctly modelling a privacy preserving mechanism such as a black-box generative model or complex noise convolution is often intractable.

This results in models that are misspecified by design, providing two insights that we explore in this paper: firstly that, when left unchecked, the Bayesian inference machine learns about the model parameters minimising the Kullback-Leibler divergence (KLD) to the synthetic data generating process (S-DGP) (Berk et al., 1966; Walker, 2013) rather than the true data generating process (DGP), and secondly that improved performance can be gained by considering robust inference methods that acknowledge this misspecification.

To achieve this, we investigate models based on a mix of simulated and real-world data to offer empirical insights on the learning procedure when a varying amount of real data is available to the user to be augmented with some unspecified amount of privatised synthetic data.

The contributions of our work can be summarised as:

1. Learning from synthetic data can lead to unpredictable outcomes, due to varying levels of model misspecification introduced by generation and privacy preservation.
2. Robust Bayesian inference offers improvements over classical Bayes when learning from synthetic data.
3. Real and synthetic data can be used in tandem to achieve practical effectiveness through the discovery of desirable stopping points for learning, and optimal model configurations.
4. Consideration of the preferred properties of the inference procedure are critical; the specific task at hand can determine how best to use synthetic data.

Throughout this research we adopt the Bayesian standpoint utilising recent developments in generalised Bayesian updating (Bissiri et al., 2016) and minimum divergence inference (Jewson et al., 2018), but note that many of the observations hold in the frequentist paradigm also.

2 Problem Formulation

We outline the inference problem as follows,

- Let $x_{1:n}$ denote a training set of n exchangeable observations from Nature’s true DGP, $F_0(x)$, such that $x_{1:n} \sim F_0(x)$; we suppose $x_i \in \mathbb{R}^d$. These real observations are held privately by a data keeper K .
- K uses data $x_{1:n}$ to produce an (ϵ, δ) -differentially private synthetic data generating mechanism (S-DGP). With a slight abuse of notation we use $\mathcal{G}_{\epsilon, \delta}(x_{1:n})$ to denote the S-DGP, noting this will cover the case where $\mathcal{G}_{\epsilon, \delta}$ is a fully generative model as well as when it involves directly privatising the finite data $x_{1:n}$ (see discussion on the S-DGP below).
- Let $f_\theta(x)$ denote a learner L ’s model likelihood for $F_0(x)$, that is parameterised by θ with prior $\tilde{\pi}(\theta)$, and marginal (predictive) likelihood $p(x) = \int_\theta f_\theta(x) \tilde{\pi}(\theta) d\theta$.
- L ’s prior may already encompass some other set of real-data drawn from F_0 leading to $\tilde{\pi}(\theta) = \pi(\theta | x_{1:n_L}^L)$, for $n_L \geq 0$ prior observations.

We adopt a decision theoretic framework (Berger, 2013), in assuming that L wishes to take some optimal action \hat{a} in a prediction or inference task; satisfying:

$$\hat{a} = \arg \max_{a \in \mathcal{A}} \int U(x, a) F_0(x) dx. \quad (2)$$

This is with respect to a user-specified utility-function $U(x, a)$ that evaluates actions in the action space \mathcal{A} , and makes precise L ’s desire to learn about F_0 in order to accurately identify \hat{a} .

Synthetic data generation mechanism. In defining $\mathcal{G}_{\epsilon, \delta}$, we believe it is important to differentiate between its two possible forms:

1. $\mathcal{G}_{\epsilon, \delta}(x_{1:n}) = G_{\epsilon, \delta}(z | x_{1:n})$, here G is a privacy-preserving generative model fit on the real data such as the PATE-GAN (Jordon et al., 2018) or DP-GAN (Xie et al., 2018). These produce differentially private synthetic data by injecting heavy-tailed noise into gradient-based learning and/or training through partitioned collections, aggregations and subsets of the data. The S-DGP provides conditional independence between $z_{1:m}$ and $x_{1:m}$ and therefore no longer queries the real data after ‘fitting’. Alternative approaches in this class include fitting Bayesian Networks (e.g. Zhang et al., 2017).
2. $\mathcal{G}_{\epsilon, \delta} = \int K_{\epsilon, \delta}(x, dz) F_0(dx)$. A special case of this integral comprises the convolution of F_0 with noise distribution H s.t $\mathcal{G}_{\epsilon, \delta} = F_0 \star H_{\epsilon, \delta}$. The sampling distribution is therefore not a function of the private data $x_{1:n}$. In this case, the number of samples that we can draw is limited to $m \leq n$ as drawing one data item requires using one sample of K ’s data. Examples of this formulation include the Laplace mechanism (Dwork et al., 2014) and transformation-based privatisation (Aggarwal and Yu, 2004).

The fundamental problem of synthetic learning is that L wants to learn about F_0 but only has access to their prior $\tilde{\pi}(\theta)$ and to $z_{1:m} \sim \mathcal{G}_{\epsilon, \delta}$, where:

- $\mathcal{G}_{\epsilon, \delta} \neq F_0$. That is, the S-DGP $\mathcal{G}_{\epsilon, \delta}(\cdot)$ is misspecified by design
- L ’s model, $p(x)$, is specified using beliefs about the target $F_0(x)$ rather than $\mathcal{G}_{\epsilon, \delta}(x)$, and the black-box nature of modern S-DGP’s makes modelling them impossible. Therefore, the posterior predictive converges to a different distribution under real and synthetic data generating processes such that $p(x | z_{1:m \rightarrow \infty}) \neq p(x | x_{1:n \rightarrow \infty})$

Learning from synthetic data is an intricate example of learning under model misspecification, where the misspecification is by K ’s design. It is important, as shown below, that this is recognised in the updating of models. Fortunately we can adapt recent advances in Bayesian inference under model misspecification to help optimise learning with respect to L ’s task.

2.1 Bayesian Inference under model misspecification

Bayesian inference under model misspecification has recently been formalised (Walker, 2013; Bissiri et al., 2016) and represents a growing area of research, see Watson and Holmes (2016); Jewson et al. (2018); Miller and Dunson (2018); Lyddon et al. (2018); Grünwald et al. (2017); Knoblauch et al. (2019) to name but a few. Traditional Bayes rule updating in this context can be seen as an approach that learns about the parameters of the model that minimises the logarithmic score, or equivalently, the Kullback-Leibler divergence (KLD) of the model from the DGP of the data (Berk et al., 1966; Walker, 2013; Bissiri et al., 2016), where $\text{KLD}(g \| f) = \int \log(g/f) d\mathcal{G}_{\varepsilon, \delta}$.

As a result, if L updates their model $f_\theta(x)$ using synthetic data $z_{1:m} \sim \mathcal{G}_{\varepsilon, \delta}(x_{1:n})$, then as $m \rightarrow \infty$ they will be learning about the limiting parameter that minimises the KLD to the S-DGP:

$$\theta_{\mathcal{G}_{\varepsilon, \delta}}^{\text{KLD}} = \arg \min_{\theta \in \Theta} \text{KLD}(g(\cdot) \| f_\theta(\cdot)), \quad (3)$$

and under regularity conditions the posterior distribution concentrates around that point, $\pi(\theta | z_{1:m}) \rightarrow \mathbf{1}_{\theta_{\mathcal{G}_{\varepsilon, \delta}}^{\text{KLD}}}$ as $m \rightarrow \infty$, where $g(\cdot)$ denotes the density function of $\mathcal{G}_{\varepsilon, \delta}$.

Moreover, the posterior will concentrate away from the model that is closest to F_0 in KLD, corresponding to the limiting model that would be learnt given an infinite real sample $x_{1:\infty}$ from F_0 :

$$\theta_{\mathcal{G}_{\varepsilon, \delta}}^{\text{KLD}} \neq \theta_{F_0}^{\text{KLD}} = \arg \min_{\theta \in \Theta} \text{KLD}(f_0(\cdot) \| f_\theta(\cdot)) \quad (4)$$

This problem is exacerbated by the injection of noise by the S-DGP to ensure (ε, δ) -DP as this process produces data $z_{1:m}$ that is prone to outliers by design, with respect to L 's model $f_\theta(x)$. So, given that as we collect more synthetic data our inference is no longer minimising the KLD towards F_0 , we must carefully consider and investigate whether our inference is still ‘useful’ for learning about F_0 at all.

2.2 The approximation to F_0

Before we proceed any further we must consider what it means for data from $\mathcal{G}_{\varepsilon, \delta}$ to be ‘useful’ for learning about F_0 . We can do so using the concepts of *scoring rules* and statistical *divergence*.

Definition 2 (Proper Scoring Rule) *The function $s : \mathcal{X} \times \mathcal{P}$ is a strictly proper scoring rule provided its difference function D satisfies*

$$D(f_0 \| f) = \mathbb{E}_{x \sim f_0} [s(x, f(\cdot))] - \mathbb{E}_{x \sim f_0} [s(x, f_0(\cdot))]$$

$D(f_1 \| f_2) \geq 0$, $D(f \| f) = 0$ for all $f, f_1, f_2 \in \mathcal{P}(x)$

$$\mathcal{P}(x) := \left\{ \int f(x) : f(x) \geq 0 \forall x \in \mathcal{X}, \int_{\mathcal{X}} f(x) dx = 1 \right\}$$

The function D measures a distance between two probability distributions. $s(x, f)$ arises as the divergence is minimised when $f_0 = f$ (Gneiting and Raftery, 2007; Dawid, 2007). A further advantage of this representation is that it allows for the minimisation of $D(f_0 \| \cdot)$ using only samples from f_0 ,

$$\begin{aligned} \arg \min_{f \in \mathcal{F}} D(f_0 \| f) &= \arg \min_{f \in \mathcal{F}} \mathbb{E}_{x \sim f_0} [s(x, f(\cdot))] \\ &\xrightarrow{n \rightarrow \infty} \frac{1}{n} \sum_{i=1}^n s(x_i, f(\cdot)), \quad x_i \sim f_0 \end{aligned} \quad (5)$$

Here, f_0 is the density of the DGP F_0 generating real data; thus the approximating density f becomes our predictive inferences made using synthetic $z_{1:m} \sim \mathcal{G}_{\varepsilon, \delta}$. Henceforth, we define any concepts of closeness (or ‘usefulness’) in terms of a chosen divergence D and associated scoring rule s . Given that inference using $\mathcal{G}_{\varepsilon, \delta}$ is no longer able to exactly capture f_0 , L can use this notion of closeness to define what aspects of F_0 they are most concerned with capturing. The importance of this specification is illustrated in Section 4.

3 Improved learning from the S-DGP

The classical assumptions underlying statistics are that minimising the KLD is the optimal way to learn about the DGP, and that more observations provide more information about this underlying DGP; such logic does not necessarily apply here. L wishes to learn about the private DGP, F_0 , but must rely on observations from the S-DGP $\mathcal{G}_{\varepsilon, \delta}$ to do so. In this section we acknowledge this setting to propose a framework for improved learning from synthetic data. In so doing we pose the following question and detail our solutions in turn: Given the scoring criteria D , is $\theta_{\mathcal{G}_{\varepsilon, \delta}}^{\text{KLD}}$ the best the learner can do?

1. Can the robustness of the *learning procedure* be improved in approximating F_0 by acknowledging the misspecification and outlier prone nature of $z_{1:m}$?
2. Starting from the prior predictive, $p(x)$, for a given learning method when does learning using $z \sim \mathcal{G}_{\varepsilon, \delta}$ stop improving inference for $F_0(x)$? That is, when

$$E_z [D(f_0(\cdot) \| p(\cdot | z_{1:j+1}))] > E_z [D(f_0(\cdot) \| p(\cdot | z_{1:j}))]$$

3.1 General Bayesian Inference

In order to address these issues we adopt a general Bayesian, minimum divergence paradigm for inference (Bissiri et al., 2016; Jewson et al., 2018) inspired by

model misspecification, where L can coherently update beliefs about their model parameter θ from prior $\pi(\theta)$ to posterior $\pi(\theta|z_{1:m})$ using:

$$\pi^\ell(\theta|z_{1:m}) \propto \frac{\tilde{\pi}(\theta) \exp(-\sum_{i=1}^m \ell(z_i, f_\theta))}{\int \tilde{\pi}(\theta) \exp(-\sum_{i=1}^m \ell(z_i, f_\theta)) d\theta}, \quad (6)$$

where $\ell(z, f_\theta)$ is the loss function used by L for inference. The logarithmic score $\ell_0(z, f_\theta) = -\log f_\theta(z)$ recovers traditional Bayes rule updating. The predictive distribution associated with such a posterior and the model f_θ is:

$$p^\ell(x|z_{1:m}) = \int f_\theta(x) \pi^\ell(\theta|z_{1:m}) d\theta \quad (7)$$

3.2 Robust Bayes and dealing with outliers

In the absence of the ability to correctly model the s-DGP, robust statistics (see e.g. Berger et al., 1994) provide an alternative option to guard against artefacts of the generated synthetic data. We can gain increased robustness in our learning procedure to data $z_{1:m}$ by changing the loss function, $\ell(z, f_\theta)$ used for inference in Eq. (6). Here we consider two alternative loss functions to the standard logarithmic score underpinning standard Bayesian statistics,

$$\ell_w(z, f_\theta) := -w \log f_\theta(z) \quad (8)$$

$$\ell^{(\beta)}(z, f_\theta) := \frac{1}{\beta+1} \int f_\theta(y)^{\beta+1} dy - \frac{1}{\beta} f_\theta(z)^\beta. \quad (9)$$

Loss function $\ell_w(z, f_\theta)$ introduces a learning parameter $w > 0$ into the Bayesian update (e.g. Lyddon et al., 2018; Grünwald et al., 2017; Miller and Dunson, 2018; Holmes and Walker, 2017). Down-weighting, $w < 1$ will generally produce a less confident posterior than in the case of traditional Bayes' rule, with a greater dependence on the prior. Conversely, $w > 1$ will have the opposite effect. The value of w can have ramifications for inference and prediction (Rossell and Rubio, 2018; Grünwald et al., 2017). However, we note that as the sample size grows using the weighted likelihood posterior will still learn about θ_G^* if w is fixed. Choosing $w = s/m$ instead averages the log-likelihood. In this case s can be seen as a notion of effective sample size.

Alternatively, minimising $\ell^{(\beta)}(x, f(\cdot))$ in expectation over the DGP is equivalent to minimising the β -divergence (β D) (Basu et al., 1998). Therefore, analogously to the KLD and the log-score, using $\ell^{(\beta)}(x, f(\cdot))$ (Bissiri et al., 2016; Jewson et al., 2018; Ghosh and Basu, 2016) produces a Bayesian update targeting:

$$\theta_{\mathcal{G}_{\varepsilon,\delta}}^{\beta D} := \arg \min_{\theta \in \Theta} \beta D(g(\cdot) \| f_\theta). \quad (10)$$

As $\beta \rightarrow 0$, then $\beta D \rightarrow \text{KLD}$, but as β increases it provides increased robustness through skepticism of

new observations relative to the prior. We demonstrate the robustness properties of the βD in some simple scenarios in the Supplementary material and refer the reader to e.g. Knoblauch et al. (2019, 2018) for further examples. We note there are many possible divergences providing greater robustness properties than the KLD, e.g. Wasserstein or Stein discrepancy (Barp et al., 2019), but for our exposition we focus on the βD for its convenience and simplicity.

A key difference between the two robust loss functions considered above is that while $\ell_w(z, f_\theta)$ down-weights the log-likelihood of each observation equally, $\ell^{(\beta)}(x, f(\cdot))$ does so adaptively, based on how likely the new observation is under the current inference (Cichocki et al., 2011). It is this adaptive down-weighting that allows the βD to target a different limiting parameter to $\theta_{\mathcal{G}_{\varepsilon,\delta}}^{\text{KLD}}$. This, in particular, allows the βD to be robust to outliers and/or heavy tailed contaminations. As a result, we believe that $D(F_0 \| f_{\theta_{\mathcal{G}_{\varepsilon,\delta}}^{\beta D}}) < D(F_0 \| f_{\theta_{\mathcal{G}_{\varepsilon,\delta}}^{\text{KLD}}})$ across a wide class of s-DGPs. That is to say that the βD minimising approximation to $\mathcal{G}_{\varepsilon,\delta}$ is a better approximation of F_0 than the KLD minimising approximation.

A strength of the βD is that, unlike standard robust methods using heavier tailed models or losses (Berger et al., 1994; Huber and Ronchetti, 1981; Beaton and Tukey, 1974), $\ell^{(\beta)}(x, f(\cdot))$ does not change the model used for inference. In the absence of any specific knowledge about the s-DGP, updating using the βD maintains the model L would have used to estimate F_0 , but updates its parameters robustly. This also has advantages in the data combination scenario where L is combining inferences from their own private data $x_{1:n_L}^L$ with synthetic data $z_{1:m}$. They can maintain the same model for both datasets, with the same model parameters, yet update robustly about $z_{1:m}$ whilst still using the log-score for $x_{1:n_L}^L$ (i.e. to produce $\tilde{\pi}(\theta)$).

3.3 The Learning Trajectory

Moreover, the concept of closeness provided by D allows us to consider how L 's approximation to F_0 changes as more data is collected from the s-DGP. Firstly, we provide a trivial theorem that says using more data and approaching the limit $\theta_{\mathcal{G}_{\varepsilon,\delta}}^{\text{KLD}}$ is not necessarily the optimal target to learn about according to criteria D .

Proposition 1 (Suboptimality of learning s-DGP)
 For s-DGP $\mathcal{G}_{\varepsilon,\delta}$, model $f_\theta(\cdot)$, and divergence D , there exists prior $\tilde{\pi}(\theta)$, private DGP F_0 and $0 \leq m < \infty$ such that

$$\mathbb{E}_z [D(F_0 \| p(\cdot|z_{1:m}))] \leq D(F_0 \| f_{\theta_{\mathcal{G}_{\varepsilon,\delta}}^{\text{KLD}}}) \quad (11)$$

where $\theta_{\mathcal{G}_{\varepsilon,\delta}}^{\text{KLD}} := \arg \min_{\theta \in \Theta} \text{KLD}(\mathcal{G}_{\varepsilon,\delta} \| f_\theta)$ and $p(x|z_{1:m})$

is the Bayesian posterior predictive distribution (using ℓ_0) based on (synthetic) data $z_{1:m}$, see Eq. (7).

The proof of Proposition 1 involves a simple counter example in which the prior is a better approximation to F_0 according to divergence D than $\mathcal{G}_{\varepsilon,\delta}$. While trivial, this could reasonably occur if L has strong, well-calibrated expert belief judgements, or if they have a considerable amount of their own data before incorporating synthetic data. Further, we argue next that by considering the path, in the number of synthetic observations m , between the prior and the s-DGP $\mathcal{G}_{\varepsilon,\delta}$ it is possible to get even ‘closer’ to F_0 . We call such a path the learning trajectory.

Changing the divergence used for inference as suggested in Section 3.2 changes these trajectories by changing their limiting parameter. However, Prop. 1, which considered learning minimising the KLD, can equally be shown for learning minimising the β D (see Supplementary material). In the following Sections we talk generally about optimising such a trajectory for a given learning method, before focusing on the comparing methods and trajectories in Section 4.

3.4 Optimising the Learning Trajectory

The insights from the previous section raise two questions for a learner L using synthetic data:

1. Is synthetic data able to improve L ’s inferences about F_0 according to divergence D ? If so,
2. What is the optimal quantity to use in getting the learner closest to F_0 according to D ?

Both questions can be solved by the estimation of

$$m^* := \arg \min_{0 \leq m \leq M} \mathbb{E}_z [D(f_0 \| p^\ell(\cdot | z_{1:m}))], \quad (12)$$

However, clearly the learner never has access to the data generating density. Instead we take advantage of the representation of proper scoring rules and propose using a ‘test set’ $x'_{1:N} \sim F_0$ to estimate

$$\hat{m} := \arg \min_{0 \leq m \leq M} \frac{1}{N} \frac{1}{B} \sum_{b=1}^B \sum_{j=1}^N s(x'_j, p^\ell(\cdot | z_{1:m}^{(b)})) \quad (13)$$

with $\{z_{1:m}^{(b)}\}_{b:1:B} \sim \mathcal{G}_{\varepsilon,\delta}$.

As such we use a small amount of data from F_0 to guide the synthetic data inference towards F_0 . We consider doing so in a tailored fashion for L ’s specific inference problem, or put the onus on K to evaluate the general ability of their s-DGP to capture F_0 .

3.4.1 Optimising for L ’s inference

Consider two potential sources of an independent test set $x'_{1:N} \sim F_0$ allowing the learner L to calculate the \hat{m} associated with the specific learning trajectory of their problem. The first option is for L to sacrifice some of their own data $x_{1:n_L}^L$ when constructing their prior. The second requires that K hold, $x'_{1:N}$ out when it trains the s-DGP, which can then be queried by L in order to estimate \hat{m} . Clearly K is not able to share the observations with L as this would violate the DP guarantee. Instead a secure protocol for two-way communication between L ’s model and K ’s test set must be established; promising directions include (Cormode et al., 2019; de Montjoye et al., 2018) and a practical use case (UK HDR Alliance, 2020).

Remark 1 We may consider data-dependent m , for a concrete stream of data $z_{1:m}$,

$$\hat{m} := \arg \min_{0 \leq m \leq M} \frac{1}{N} \sum_{j=1}^N s(x'_j, p^\ell(\cdot | z_{1:m})). \quad (14)$$

This introduces an undesirable dependency on the ordering of the data but can be mitigated by averaging different realisations of the synthetic data, which in turn can be shown to improve any convex proper scoring rule, see Prop. 2. See the Supplementary material for a proof of this Remark.

3.4.2 A Broader Study

When the previous, problem and data specific methods are not available we have to fall back on a broader study. Here we recommend that alongside releasing synthetic data, K optimises the learning trajectory themselves, under some default model, loss and prior setting by repeatedly partitioning $x_{1:n}$ into test and training sets. For example, when releasing classification data, K could release an \hat{m} associated with logistic regression and BART, for the log-score, under some vaguely informative priors, providing learners an idea of what to expect. While this is less tailored to any specific inference problem it still allows K to communicate a broad measure of the quality of its synthetic data for learning about F_0 .

3.5 Posthoc improvement through averaging

If more synthetic data is available (e.g. sampling $z_{1:m}, m \rightarrow \infty$ from a GAN), we can average the posterior predictive distribution across different realisations ensuring we do not waste synthetic data when \hat{m} is less than the maximum available. Jensen’s inequality allows us to improve the performance of the predictive distribution if we consider convex proper scoring rules such as the logarithmic score:

Proposition 2 (Predictive Averaging) *Given divergence D with convex scoring rule, averaging over different realisations of the posterior predictive depending on different synthetic data sets improves inference by Jensen’s inequality:*

$$\begin{aligned} \mathbb{E}_z D \left(F_0 \parallel \frac{1}{B} \sum_{b=1}^B \tilde{p} \left(x | z_{1:m}^{(b)} \right) \right) &\leq \\ \mathbb{E}_z \frac{1}{B} \sum_{b=1}^B D \left(F_0 \parallel \tilde{p} \left(x | z_{1:m}^{(b)} \right) \right) &= \\ \mathbb{E}_z D \left(F_0 \parallel \tilde{p} \left(x | z_{1:m}^{(b)} \right) \right). & \end{aligned}$$

The significance of this is that more synthetic data can always be used to improve the predictive distribution, but not by naïvely using all of it to learn at once.

4 Experimental Setup and Results

In order to investigate the concepts and methodologies outlined above, we consider two experiment types:

1. Learning the location and variance of a Gaussian distribution.
2. Using Bayesian logistic regression for binary classification on a selection of real-world datasets.

In these contexts we investigate the learning trajectory of classical Bayesian updating alongside the robust adjustments discussed in Section 3.2. In order to draw comparisons between these methods, we study the trajectories’ dependence on values spanning a grid of data quantities n_L and m , robustness parameters w and β , prior values, and the parameters of chosen DP mechanisms (Full experiment specifications are included in the Supplementary material). The varying amounts of unprivatised data available to L were used to construct increasingly informative priors $\tilde{\theta} = \pi(\theta | x_{1:n_L}^L)$, using standard Bayesian updating as no robustness is required when learning using data from F_0 . Learning trajectories are then estimated utilising an unseen dataset $x'_{1:N}$ (mimicking that defined by either K ’s data or some subset of L ’s data not used in training).

To this end we use optimised MCMC sampling schemes (e.g. Hoffman and Gelman, 2014) to sample from the classical and adjusted posteriors in each case and draw comparisons across the grid laid out above, repeating experiments to mitigate any sources of noise. This results in an extensive computational task, made feasible through a mix of Julia’s Turing PPL (Ge et al., 2018), MLJ (Blaom et al., 2020) and Stan (Carpenter et al., 2017).

The majority of the experiments are carried out with $\varepsilon = 6$, which is seen to be a realistic value respective of

practical applications (Lee and Clifton, 2011; Erlingson et al., 2014; Tang et al., 2017; Differential Privacy Team at Apple, 2017) and upon observation of the relationship between privacy and misspecification shown in the figure included in the Supplementary material.

4.1 Simulated Gaussian Models

We first introduce a simple but illustrative simulated example in which we infer the parameters of a Gaussian model $f_\theta = \mathcal{N}(\mu, \sigma^2)$ where $\theta = (\mu, \sigma^2)$. We place conjugate priors on θ with $\sigma^2 \sim \text{InverseGamma}(\alpha_p, \beta_p)$ and $\mu \sim \mathcal{N}(\mu_p, \sigma_p * \sigma)$ respectively. We consider $x_{1:n}$ drawn from DGP $F_0 = \mathcal{N}(0, 1^2)$ and adopt the Laplace mechanism (Dwork et al., 2014) to define our S-DGP. This perturbs samples drawn from the DGP with noise drawn from the Laplace distribution of scale λ , calibrated via the sensitivity \mathcal{S} of the DGP in order to provide $(\varepsilon, 0)$ -DP per the Laplace mechanism’s definition with $\varepsilon = \mathcal{S}/\lambda$. To achieve finiteness of \mathcal{S} in this case, we adjust our model to be that of a truncated Gaussian; restricting its range to $\pm 3\sigma$ to allow for meaningful ε ’s to be calculated under the Laplace mechanism.

We then compare and evaluate the empirical performances of the models defined below (formulations are given explicitly in the Supplementary material):

1. The standard likelihood formulated with a w parameter as in Eq. (8).
2. The posterior under the βD loss as in Eq. (9).
3. The ‘Noise-Aware’ likelihood where the S-DGP can be tractably modelled using the Normal-Laplace convolution (Reed, 2006; Amini and Rabbani, 2017).

4.1.1 Results and Discussion

We observe that three different categories of learning trajectory occur across the models, these are illustrated in the ‘branching’ plots in Figure 1:

1. The prior $\tilde{\pi}$ is sufficiently inaccurate or uninformative (in this case due to low n_L) such that the synthetic data continues to be useful across the range of m we consider. As a result the learning trajectory is a monotonically decreasing curve in the criteria of interest.
2. A turning point is observed; synthetic data initially brings us closer to F_0 before further synthetic data moves the inference away. We see that in the majority of cases these trajectories lie under the limiting KLD and βD approximations to $\mathcal{G}_{\varepsilon, \delta}$ demonstrating the efficacy of ‘optimising the learning trajectory’.
3. The final scenario occurs under a sufficiently informative prior $\tilde{\pi}$ (here due to large n_L) such that synthetic data is not observably of any use at all and immediately causes the model to perform worse.

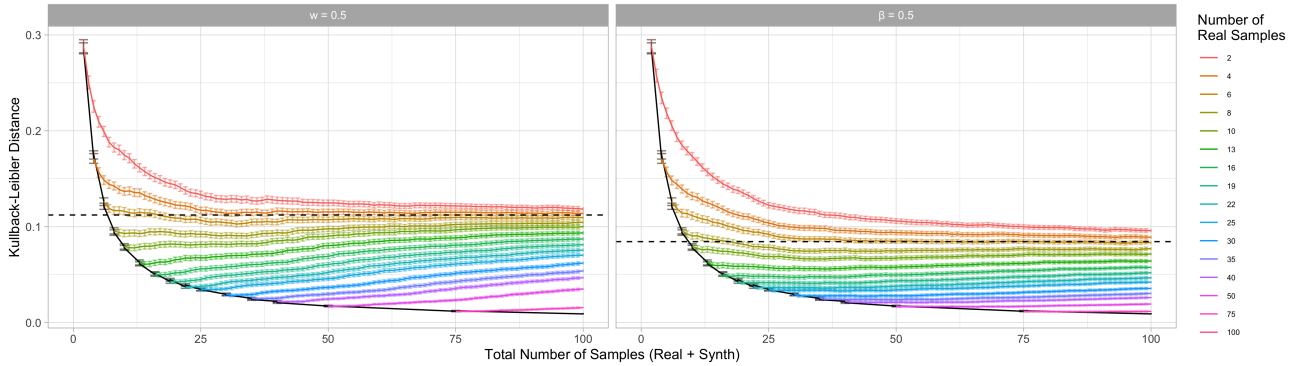


Figure 1: Shows how the KLD to F_0 changes as we add more synthetic data, starting with increasing amount of real data. This demonstrates the effectiveness of the best β D configuration found compared to the the closest alternative traditional model in terms of performance with down-weighting $w = 0.5$; the black dashed line represents $\text{KLD}(F_0 \| f_{\theta^*})$ for $\theta^* = \theta_{\mathcal{G}_{\epsilon, \delta}}^{\text{KLD}}$ on the left and $\theta^* = \theta_{\mathcal{G}_{\epsilon, \delta}}^{\beta\text{D}}$ on the right, representing the approximation to F_0 given an infinite sample from $\mathcal{G}_{\epsilon, \delta}$ under the two learning methods.

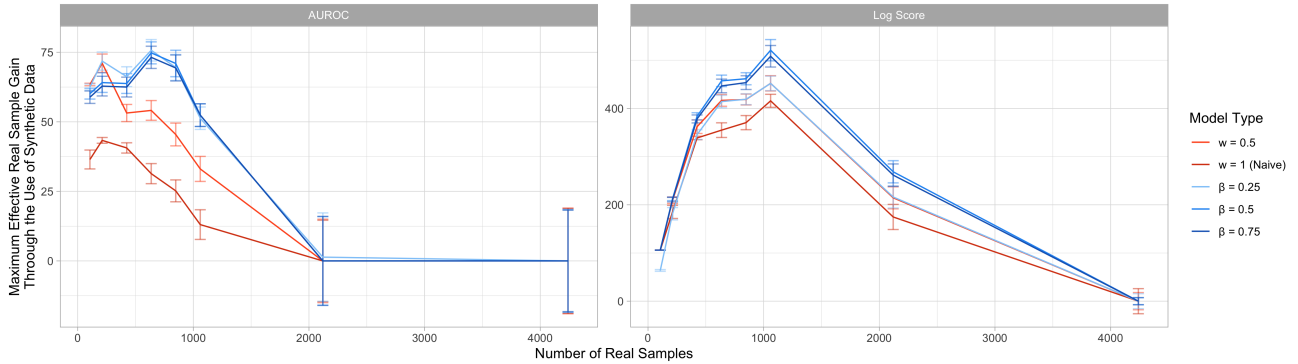
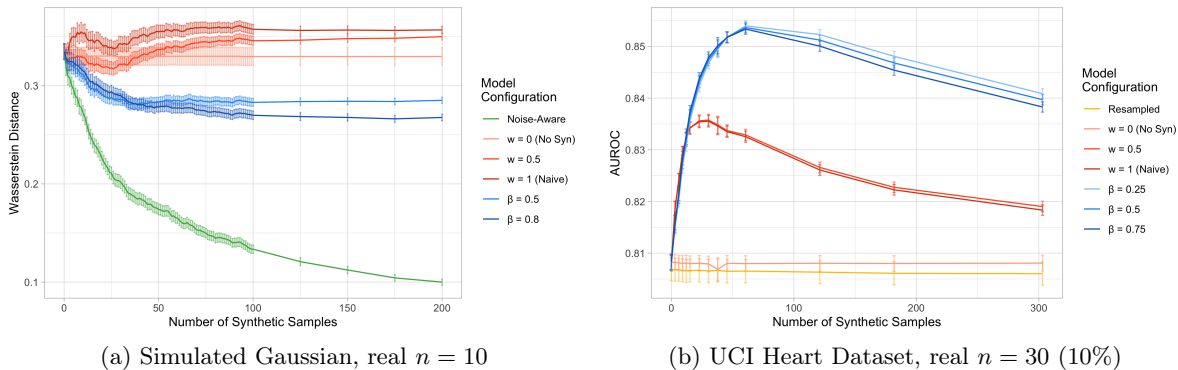


Figure 2: Shows the effective number of real samples gained through optimal \hat{m} synthetic observations alongside varying amounts of real data usage w.r.t the AUROC and log-score performance criteria. These are calculated and presented here via bootstrapped averaging under a logistic regression model learnt on the Framingham dataset. The amount of effective real samples is significantly affected by the learning task’s focused criteria.



(a) Simulated Gaussian, real $n = 10$

(b) UCI Heart Dataset, real $n = 30$ (10%)

Figure 3: Given a fixed real amount of data, we can compare model performances directly by focusing on one of the ‘branches’ in the class of diagrams shown in Figures 1 & 4, to see that the β D’s performance falls between that of the noise-aware model and the other models, exhibiting robust and desirable behaviour across a range of β . Naïve and reweighting-based approaches fail to gain significantly over not using synthetic data (shown by $w = 0$ ’s flat trajectory); the resampled model in the logistic case can also be seen to perform very poorly in comparison to models that leverage the synthetic data.

We can further quantify what is perhaps the most interesting characteristic of these experiments: the turning points. To do this we formulate bootstrapped averages of the number of ‘effective real samples’ that correspond to the estimated optimal quantity of synthetic data. This is done by comparing these minima with the black curves in the ‘branching’ plots representing the learning trajectory under an increasing n_L and $m = 0$. These calculations are shown in Figure 2; the Supplementary contains more details.

In general, we observe a significant increase in performance from the β_D (see Figures 1, 3), indicated by its proximity to even the noise-aware model at lower values of n_L , and more modest improvements from reweighting methods. The β_D achieves more desirable minimum-trajectory log score, KLD and Wasserstein values in the majority of cases compared to the other model types, and also exhibits greater robustness to larger amounts of synthetic data where other approaches can lose out significantly.

4.2 Logistic Regression

We now move on to a more prevalent and practical class of models that also exhibit the potentially dangerous behaviours of synthetic data in a real-world scenario on datasets concerning subjects that have legitimate potential privacy concerns. Namely, we build logistic regression models for the UCI Heart Disease dataset (Dua and Graff, 2017) and the Framingham Cohort dataset (Splansky et al., 2007). Clearly, we are now only able to access the empirical distribution F_n^* , where n^* is the total amount of data present in each dataset. We use $x_{1:n^*}$ to train an instance of the aforementioned PATE-GAN $\mathcal{G}_{\epsilon,\delta}$ and keep back $x_{1:(n^*-n^*)}$ for evaluation; we then draw synthetic data samples $z_{1:m} \sim \mathcal{G}_{\epsilon,\delta}$. As before, we investigate how the learning trajectories are affected across the experimental parameter grid.

Again we consider learning using ℓ_w and ℓ_β applied to the logistic regression likelihood, f_θ (the exact formulations of these are provided in the Supplement). In this case we cannot formulate a ‘Noise-Aware’ model due to the black-box nature of the GAN; this highlights the reality of the model misspecification setting we find ourselves in outside of simple simulated examples, but can instead define a ‘resampled’ model that recycles the real data in the prior.

4.2.1 Results and Discussion

Here the learning trajectories are defined with respect to the AUROC as well as the log score; whilst not technically a divergence this gives us a decision theoretic criteria to quantify the closeness of our inference to F_0 . Referring to Figures 2, 3 and 4 we see that

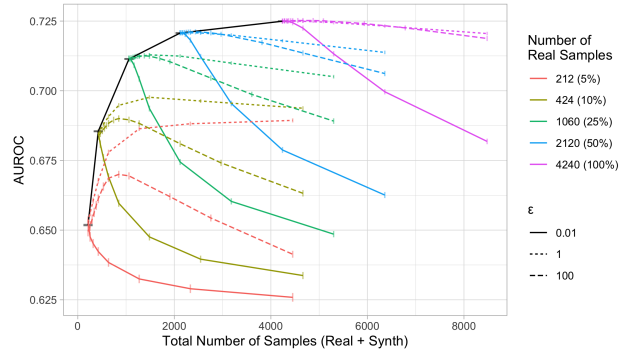


Figure 4: This plot illustrates an interesting and important observation made when varying ϵ for a GAN based model, we observe that there is a privacy ‘sweet-spot’ around $\epsilon = 1$ whereby more private data performs better than less private data (see the curves for $\epsilon = 100$).¹

the learning trajectories observed in this more realistic example mirror those observed in our simulated Gaussian experiments. There are however some cases in which the reweighted posterior outperforms the β_D , and importantly we see large discrepancies in \hat{m} when comparing log score to AUROC values meaning the learning task is critical to define.

One particularly interesting observation unique to experiments using synthetic data from a GAN is that: we see an improvement in performance as epsilon decreases up to a point. We believe this is due to potential mode collapse in the GAN learning process on imbalanced datasets, and concentration of $\mathcal{G}_{\epsilon,\delta}$ as the injected noise increases such that a small number of synthetic samples can actually be *more* representative of F_0 than even the real data. This effect is short lived as presumably these samples then become over-represented through the posterior distribution and performance begins to fall off, see Figure 4.

5 Conclusions

We consider foundations of Bayesian learning from synthetic data that acknowledge the intrinsic model misspecification and learning task at hand. Contrary to traditional statistical inferences, conditioning on increasing amounts of synthetic data is not guaranteed to help you learn about the true data generating process or make better decisions. Down-weighting the information in synthetic data (either using a weight w or divergence β_D) provides a principled approach to robust optimal information processing and warrants further investigation.

¹This plot exhibits the effect under the β_D model on the Framingham dataset with $\beta = 0.5$, but is observable across all model types in both AUROC and log score.

Acknowledgements

HW is supported by the Feuer International Scholarship in Artificial Intelligence. JJ was funded by the Ayudas Fundación BBVA a Equipos de Investigación Científica 2017 and Government of Spain’s Plan Nacional PGC2018-101643-B-I00 grants whilst working on this project. SJV is supported by The Alan Turing Institute (EPSRC grant EP/N510129/) and the University of Warwick IAA funding. CH is supported by The Alan Turing Institute, Health Data Research UK, the Medical Research Council UK, the Engineering and Physical Sciences Research Council (EPSRC) through the Bayes4Health programme Grant EP/R018561/1, and AI for Science and Government UK Research and Innovation (UKRI).

References

- Charu C Aggarwal and Philip S Yu. A condensation approach to privacy preserving data mining. In *Advances in Database Technology - EDBT 2004*, pages 183–199. Springer Berlin Heidelberg, 2004.
- Zahra Amini and Hossein Rabbani. Letter to the editor: Correction to “the normal-laplace distribution and its relatives”. *Communications in Statistics-Theory and Methods*, 46(4):2076–2078, 2017.
- Alessandro Barp, Francois-Xavier Briol, Andrew Duncan, Mark Girolami, and Lester Mackey. Minimum stein discrepancy estimators. In *Advances in Neural Information Processing Systems*, pages 12964–12976, 2019.
- Ayanendranath Basu, Ian R Harris, Nils L Hjort, and MC Jones. Robust and efficient estimation by minimising a density power divergence. *Biometrika*, 85(3):549–559, 1998.
- Albert E Beaton and John W Tukey. The fitting of power series, meaning polynomials, illustrated on band-spectroscopic data. *Technometrics*, 16(2):147–185, 1974.
- James O Berger. *Statistical Decision Theory and Bayesian Analysis*. Springer Science & Business Media, March 2013.
- James O Berger, Elías Moreno, Luis Raul Pericchi, M Jesús Bayarri, José M Bernardo, Juan A Cano, Julián De la Horra, Jacinto Martín, David Ríos-Insúa, Bruno Betrò, et al. An overview of robust bayesian analysis. *Test*, 3(1):5–124, 1994.
- Robert H Berk et al. Limiting behavior of posterior distributions when the model is incorrect. *The Annals of Mathematical Statistics*, 37(1):51–58, 1966.
- José M Bernardo and Adrian FM Smith. Bayesian theory, 2001.
- Garrett Bernstein and Daniel R Sheldon. Differentially private bayesian inference for exponential families. In *Advances in Neural Information Processing Systems*, pages 2919–2929, 2018.
- Garrett Bernstein and Daniel R Sheldon. Differentially private bayesian linear regression. In *Advances in Neural Information Processing Systems*, pages 523–533, 2019.
- PG Bissiri, CC Holmes, and Stephen G Walker. A general framework for updating belief distributions. *Journal of the Royal Statistical Society: Series B (Statistical Methodology)*, 2016.
- Anthony D Blaom, Franz Kiraly, Thibaut Lienart, Yianis Simillides, Diego Arenas, and Sebastian J Vollmer. MLJ: A Julia package for composable Machine Learning. July 2020.
- Bob Carpenter, Andrew Gelman, Matthew D Hoffman, Daniel Lee, Ben Goodrich, Michael Betancourt, Marcus Brubaker, Jiqiang Guo, Peter Li, and Allen Riddell. Stan: A probabilistic programming language. *Journal of statistical software*, 76(1), 2017.
- Andrzej Cichocki, Sergio Cruces, and Shun-ichi Amari. Generalized alpha-beta divergences and their application to robust nonnegative matrix factorization. *Entropy*, 13(1):134–170, 2011.
- Graham Cormode, Tejas Kulkarni, and Divesh Srivastava. Answering range queries under local differential privacy, 2019.
- A Philip Dawid. The geometry of proper scoring rules. *Annals of the Institute of Statistical Mathematics*, 59(1):77–93, 2007.
- Yves-Alexandre de Montjoye, Sébastien Gams, Vincent Blondel, Geoffrey Canright, Nicolas de Cordes, Sébastien Deletaille, Kenth Engø-Monsen, Manuel Garcia-Herranz, Jake Kendall, Cameron Kerry, Gautier Krings, Emmanuel Letouzé, Miguel Luengo-Oroz, Nuria Oliver, Luc Rocher, Alex Rutherford, Zbigniew Smoreda, Jessica Steele, Erik Wetter, Alex Sandy Pentland, and Linus Bengtsson. On the privacy-conscious use of mobile phone data. *Sci Data*, 5: 180286, December 2018.
- Differential Privacy Team at Apple. Learning with privacy at scale. 2017.
- Dheeru Dua and Casey Graff. UCI machine learning repository, 2017.
- Cynthia Dwork and Jing Lei. Differential privacy and robust statistics. In *Proceedings of the forty-first annual ACM symposium on Theory of computing*, pages 371–380, 2009.
- Cynthia Dwork, Frank McSherry, Kobbi Nissim, and Adam Smith. Calibrating noise to sensitivity in

- private data analysis. In *Theory of cryptography conference*, pages 265–284. Springer, 2006.
- Cynthia Dwork, Aaron Roth, et al. The algorithmic foundations of differential privacy. *Foundations and Trends in Theoretical Computer Science*, 9(3-4):211–407, 2014.
- Úlfar Erlingsson, Vasyl Pihur, and Aleksandra Korolova. Rappor: Randomized aggregatable privacy-preserving ordinal response. In *Proceedings of the 2014 ACM SIGSAC conference on computer and communications security*, pages 1054–1067, 2014.
- Hong Ge, Kai Xu, and Zoubin Ghahramani. Turing: a language for flexible probabilistic inference. In *International Conference on Artificial Intelligence and Statistics, AISTATS 2018, 9-11 April 2018, Playa Blanca, Lanzarote, Canary Islands, Spain*, pages 1682–1690, 2018. URL <http://proceedings.mlr.press/v84/ge18b.html>.
- Abhik Ghosh and Ayanendranath Basu. Robust bayes estimation using the density power divergence. *Annals of the Institute of Statistical Mathematics*, 68(2):413–437, 2016.
- Tilmann Gneiting and Adrian E Raftery. Strictly proper scoring rules, prediction, and estimation. *Journal of the American Statistical Association*, 102(477):359–378, 2007.
- Ian Goodfellow, Jean Pouget-Abadie, Mehdi Mirza, Bing Xu, David Warde-Farley, Sherjil Ozair, Aaron Courville, and Yoshua Bengio. Generative adversarial nets. In *Advances in neural information processing systems*, pages 2672–2680, 2014.
- Peter Grünwald, Thijs Van Ommen, et al. Inconsistency of bayesian inference for misspecified linear models, and a proposal for repairing it. *Bayesian Analysis*, 12(4):1069–1103, 2017.
- Matthew D Hoffman and Andrew Gelman. The no-u-turn sampler: adaptively setting path lengths in hamiltonian monte carlo. *J. Mach. Learn. Res.*, 15(1):1593–1623, 2014.
- CC Holmes and SG Walker. Assigning a value to a power likelihood in a general bayesian model. *Biometrika*, 104(2):497–503, 2017.
- Peter J Huber and EM Ronchetti. Robust statistics, series in probability and mathematical statistics, 1981.
- Jack Jewson, Jim Smith, and Chris Holmes. Principles of Bayesian inference using general divergence criteria. *Entropy*, 20(6):442, 2018.
- James Jordon, Jinsung Yoon, and Mihaela van der Schaar. Pate-gan: Generating synthetic data with differential privacy guarantees. In *International Conference on Learning Representations*, 2018.
- Jeremias Knoblauch, Jack Jewson, and Theodoros Damoulas. Doubly robust Bayesian inference for non-stationary streaming data using β -divergences. In *Advances in Neural Information Processing Systems (NeurIPS)*, pages 64–75, 2018.
- Jeremias Knoblauch, Jack Jewson, and Theodoros Damoulas. Generalized variational inference. *arXiv preprint arXiv:1904.02063*, 2019.
- Jaewoo Lee and Chris Clifton. How much is enough? choosing ϵ for differential privacy. In *International Conference on Information Security*, pages 325–340. Springer, 2011.
- SP Lyddon, CC Holmes, and SG Walker. General bayesian updating and the loss-likelihood bootstrap. *Biometrika*, 2018.
- Jeffrey W Miller and David B Dunson. Robust bayesian inference via coarsening. *Journal of the American Statistical Association*, pages 1–13, 2018.
- William J Reed. The normal-laplace distribution and its relatives. In *Advances in distribution theory, order statistics, and inference*, pages 61–74. Springer, 2006.
- Luc Rocher, Julien M Hendrickx, and Yves-Alexandre De Montjoye. Estimating the success of re-identifications in incomplete datasets using generative models. *Nature communications*, 10(1):1–9, 2019.
- David Rossell and Francisco J Rubio. Tractable bayesian variable selection: beyond normality. *Journal of the American Statistical Association*, 113(524):1742–1758, 2018.
- Greta Lee Splansky, Diane Corey, Qiong Yang, Larry D Atwood, L Adrienne Cupples, Emelia J Benjamin, Ralph B D’Agostino Sr, Caroline S Fox, Martin G Larson, Joanne M Murabito, et al. The third generation cohort of the national heart, lung, and blood institute’s framingham heart study: design, recruitment, and initial examination. *American journal of epidemiology*, 165(11):1328–1335, 2007.
- Jun Tang, Aleksandra Korolova, Xiaolong Bai, Xueqiang Wang, and Xiaofeng Wang. Privacy loss in apple’s implementation of differential privacy on macos 10.12. *arXiv preprint arXiv:1709.02753*, 2017.
- The Royal Society. Privacy Enhancing Technologies: protecting privacy in practice. 2019.
- UK HDR Alliance. Trusted research environments (TRE). https://ukhealthdata.org/wp-content/uploads/2020/07/200723-Alliance-Board_Paper-E_TRE-Green-Paper.pdf, 2020. Accessed: 2020-10-15.
- Stephen G Walker. Bayesian inference with misspecified models. *Journal of Statistical Planning and Inference*, 143(10):1621–1633, 2013.

James Watson and Chris Holmes. Approximate models and robust decisions. *Statistical Science*, 31(4):465–489, 2016.

Liyang Xie, Kaixiang Lin, Shu Wang, Fei Wang, and Jiayu Zhou. Differentially private generative adversarial network. *arXiv preprint arXiv:1802.06739*, 2018.

Jun Zhang, Graham Cormode, Cecilia M Procopiuc, Divesh Srivastava, and Xiaokui Xiao. PrivBayes: Private data release via bayesian networks. *ACM Trans. Database Syst.*, 42(4):1–41, October 2017.

A.1 The β -Divergence

The β -divergence (βD) was first introduced by Basu et al. (1998) under the name ‘density power divergence’, as a robust and efficient alternative to frequentist maximum-likelihood estimation. It has since been used to produce Bayesian posteriors, firstly in Ghosh and Basu (2016) before being unified by generalised Bayesian updating (Bissiri et al., 2016) in Jewson et al. (2018). Recent applications of the βD are vast, representing a growing area of research.

The β -divergence between two distributions with densities g and f with dominating measure μ (which we in general assume to be the Lebesgue measure) is

$$\beta\text{D}(g \| f) := \frac{1}{\beta + 1} \int f^{\beta+1} d\mu - \frac{1}{\beta} \int f^\beta g d\mu + \frac{1}{\beta(\beta + 1)} \int g^{\beta+1} d\mu. \quad (\text{A.1})$$

When minimising $\beta\text{D}(g \| f_\theta)$ for θ , the final term $\frac{1}{\beta(\beta+1)} \int g^{\beta+1} d\mu$ can be ignored and therefore

$$\theta_G^{\beta\text{D}} := \operatorname{argmin}_{\theta \in \Theta} \beta\text{D}(g \| f_\theta) = \operatorname{argmin}_{\theta \in \Theta} \mathbb{E}_{z \sim g} \left[\ell^{(\beta)}(z, f_\theta) \right], \quad (\text{A.2})$$

with the law of large numbers providing that only a sample $\{x_i\}_{1:n} \sim g$ is needed to instantiate such a minimiser

$$\mathbb{E}_{z \sim g} \left[\ell^{(\beta)}(z, f_\theta) \right] \xrightarrow[n \rightarrow \infty]{} \frac{1}{n} \sum_{i=1}^n \ell^{(\beta)}(z_i, f_\theta), \quad x_i \sim g, \quad (\text{A.3})$$

and from Eq. (9) of the main paper

$$\ell^{(\beta)}(z, f_\theta) := \frac{1}{\beta + 1} \int f_\theta(y)^{\beta+1} dy - \frac{1}{\beta} f_\theta(z)^\beta.$$

The fact that

$$\lim_{\beta \rightarrow 0} \frac{1}{\beta} x^\beta = \log x, \quad (\text{A.4})$$

is then enough to prove that $\lim_{\beta \rightarrow 0} \beta\text{D} = \text{KLD}$.

A.1.1 The Robustness of the βD

This section provides some illustrations demonstrating the robustness of the general Bayesian update using $\ell_w(x, f_\theta)$ and $\ell^{(\beta)}(x, f_\theta)$ compared with traditional Bayesian updating (using $\ell_0(x, f_\theta)$).

Firstly we consider how observations are ‘downweighted’ compared with the prior under different learning / updating procedures. First, we let the model be a Gaussian location scale model $f_\theta = \mathcal{N}(\mu, \sigma^2)$. We start with a conjugate Normal-Inverse-Gamma (NIG) prior, $NIG(\mu, \sigma^2; a_0, b_0, \mu_0, \kappa_0) = \mathcal{IG}(\sigma^2; a_0, b_0) \times \mathcal{N}(\mu; \mu_0, \sigma^2 / \kappa_0)$ with $(a_0, b_0, \mu_0, \kappa_0) = (2, 1, 0, 1/2)$ and consider the posterior after observing an observation ‘in agreement’ with the prior $x_{in} = 0.5$ and one not in agreement with the prior $x_{out} = 5$. Figure A.1, plots the prior and posterior predictives’ densities after observing one observation in these two cases.

After seeing an ‘inlying’ observation consistent with the prior, all three methods learn similarly, with their posterior predictives’ modes being shifted towards the observation. However, we see that using either $\ell_w(x, f_\theta)$ or $\ell^{(\beta)}(x, f_\theta)$ gives more relative weight to the prior than traditional Bayesian updating, as they continue to produce larger posterior variances driven by the prior. After seeing an ‘outlier’ the three methods produce very different inferences. One outlying observation can be seen to move the traditional Bayesian inference away from the prior predictive; the same effect is witnessed when using $\ell_w(x, f_\theta)$, although to a lesser extent in that the posterior predictive also carries a large variance compared to the traditional Bayesian one. Inference under the βD is very different given an outlier. The posterior predictive mode stays in agreement with the prior but the right tail of the posterior is heavier than the left in order to ‘acknowledge’ the outlying observation.

Next we formalise the influence (Kurtek and Bharath, 2015; Jewson et al., 2018) given to different observations under the different learning methods, $\ell_w(x, f_\theta)$ and $\ell^{(\beta)}(x, f_\theta)$ w.r.t the Gaussian model $f_\theta = \mathcal{N}(\mu, \sigma^2)$. Here

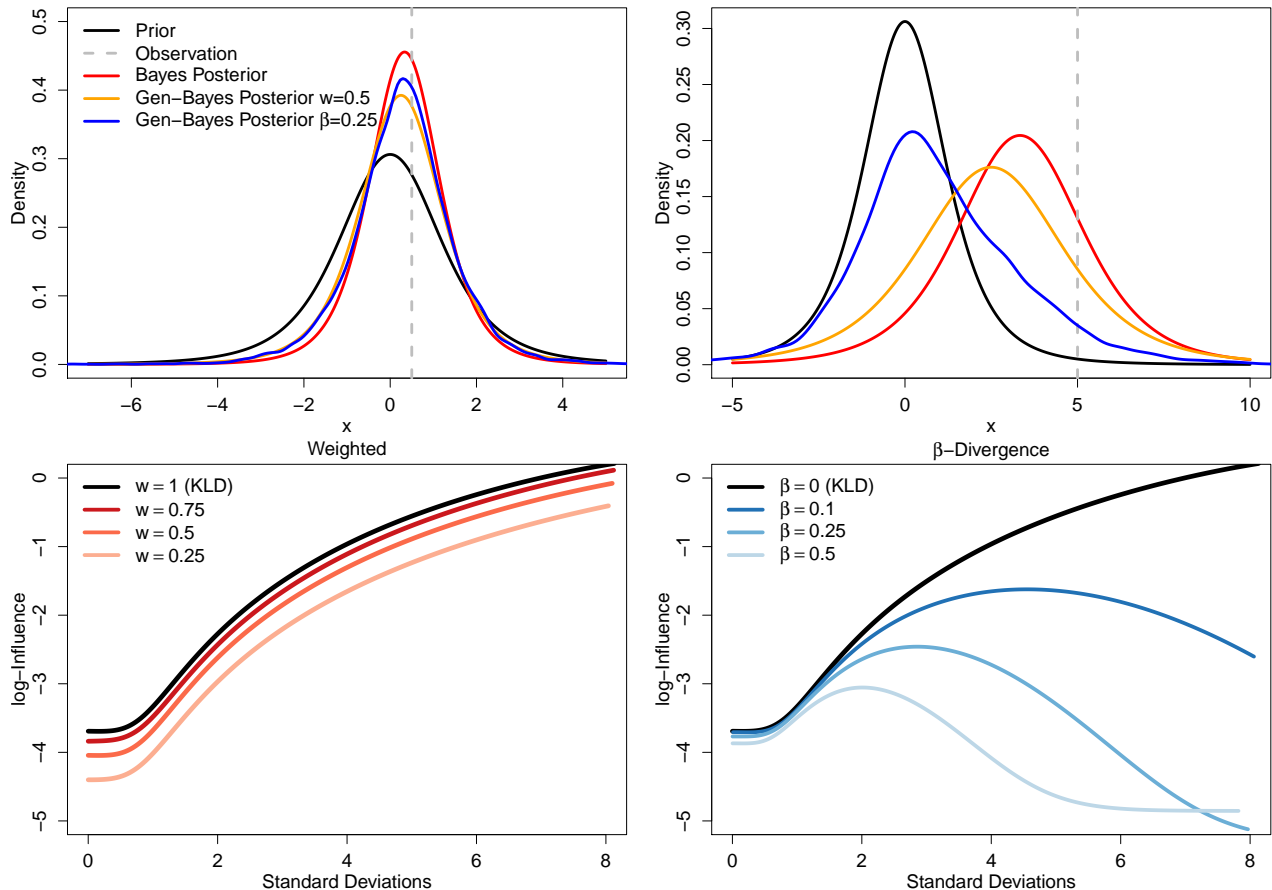


Figure A.1: Influence of Outliers. **Top:** NIG Prior predictive (**black**) and posterior predictives using a Gaussian model, $f_\theta = \mathcal{N}(\mu, \sigma^2)$, under traditional Bayesian updating ($\ell_0(x, f_\theta)$) (**red**) and general Bayesian updating with $\ell_w(x, f_\theta)$ (**orange**) and $\ell^{(\beta)}(x, f_\theta)$ (**blue**) after an inlying (**Left**) and outlying (**Right**) observation (**grey**). **Bottom:** log-Fisher-Rao-metric (Kurtek and Bharath, 2015) between the general Bayesian posterior with or without one observation at different posterior standard deviations away from the previous posterior mean for $\ell_w(x, f_\theta)$ (**Left**) and $\ell^{(\beta)}(x, f_\theta)$ (**Right**) under model $f_\theta = \mathcal{N}(\mu, \sigma^2)$.

we examine $R(\pi^{\ell(\theta|z_{1:n}, x)}, \pi^{\ell(\theta|z_{1:n})})$: the Fisher-Rao metric between the general Bayesian posterior based on observations $\{z_{1:n}, x\}$ and the general Bayesian posterior based only on $z_{1:n}$, providing an idea of how an observation at x influences the posterior. Figure A.1 shows this for variable x , loss functions $\ell_w(x, f_\theta)$ and $\ell^{(\beta)}(x, f_\theta)$ for varying w and β , and $z_{1:n} \sim \mathcal{N}(0, 1)$ with $n = 200$. The influence plots under $\ell_w(x, f_\theta)$ are monotonically increasing, showing that as an observation becomes less likely under the current inference its influence over the analysis increases. Decreasing $w < 1$ decreases the influence of a new observation, but we can see this happens uniformly meaning an outlier is downweighted by the same amount as an observation near the current posterior mode. Under $\ell^{(\beta)}(x, f_\theta)$ the influence curves are no longer monotonic as the observation moves away from the current posterior mean. Initially, the influence of observations increases, mimicking inference under $\ell_w(x, f_\theta)$, but then after a point the influence starts to decrease as these observations become increasingly unlikely given the current inference. This allows β D-inference to adaptively reject the influence of outliers.

Lastly we show how the downweighting of the influence of observations illustrated above affects inference for large samples. We consider inference for a Gaussian model $f_\theta = \mathcal{N}(\mu, \sigma^2)$ based on two datasets of size $n = 1000$ generated from $g_1(x) = 0.9\mathcal{N}(0, 1^2) + 0.1\mathcal{N}(5, 3^2)$ and $g_2(x) = \mathcal{L}(0, 1)$. Generating process g_1 is referred to as an ϵ -contamination, where the model is correct for $(1 - \epsilon)\%$ of observations but is contaminated with $\epsilon\%$ outliers, whilst g_2 has heavier tails than f_θ . Figure A.2 plots the posterior predictive approximation of both g_1 and g_2 for traditional Bayesian updating and general Bayesian updating with $\ell_w(x, f_\theta)$ and $\ell^{(\beta)}(x, f_\theta)$. Firstly, for $n = 1000$ there is little difference between the traditional Bayesian inference and the general Bayesian inference using

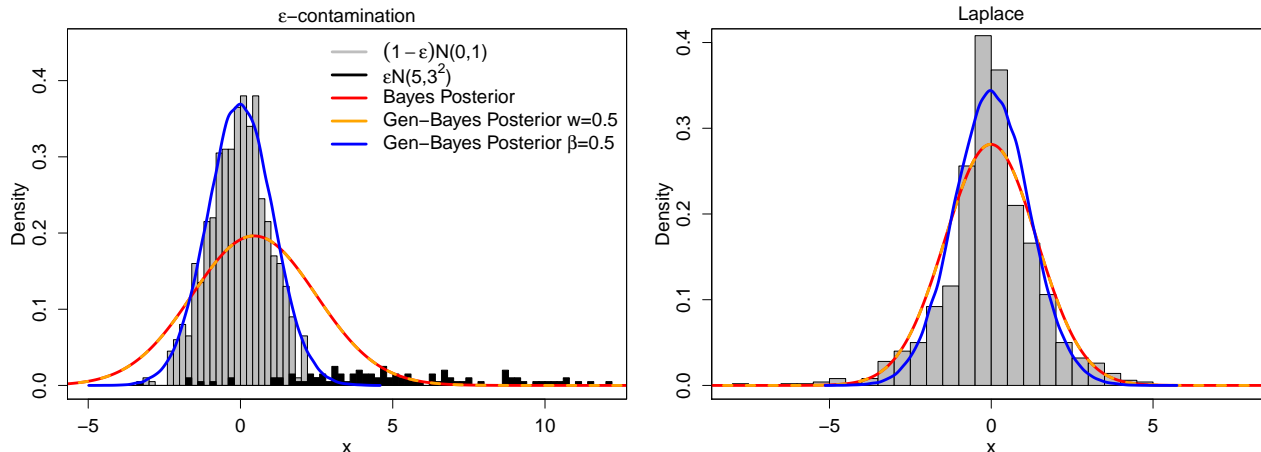


Figure A.2: General Bayesian Predictive densities from $\ell_0(x, f_\theta)$ (red), $\ell_w(x, f_\theta)$ (orange) and $\ell^{(\beta)}(x, f_\theta)$ (blue) given $n = 1000$ observations from $g_1(x) = 0.9\mathcal{N}(0, 1^2) + 0.1\mathcal{N}(5, 3^2)$ (Left) and $g_2(x) = \text{Laplace}(0, 1)$ (Right) under model $f_\theta = \mathcal{N}(\mu, \sigma^2)$

$\ell_w(x, f_\theta)$. Additionally we see that minimising the β D allows the general Bayesian inference to be less concerned with correctly capturing the tails of g_1 and g_2 and as a result allows it to provide a more accurate approximation to their modes.

A.2 Proof of Propositions

A.2.1 Proof of Proposition 1

Next we prove that for a given S-DGP $\mathcal{G}_{\varepsilon, \delta}$, model $f(\cdot; \theta)$ and infinite synthetic data sample $z_{1:\infty} \sim \mathcal{G}_{\varepsilon, \delta}$, there exists prior $\pi(\theta)$ and private DGP F_0 such that the L is able to get closer to F_0 in terms of D , than if they were to use the KLD limiting approximation to S-DGP $\mathcal{G}_{\varepsilon, \delta}$ $\theta_{\mathcal{G}_{\varepsilon, \delta}}^{\text{KLD}}$

Proposition 1 (Suboptimality of learning from the S-DGP). *For S-DGP $\mathcal{G}_{\varepsilon, \delta}$, model $f_\theta(\cdot)$, and divergence D , there exists prior $\tilde{\pi}(\theta)$, private DGP F_0 and $0 \leq m < \infty$ such that*

$$\mathbb{E}_z [D(F_0 \| p(\cdot | z_{1:m}))] \leq D\left(F_0 \| f_{\theta_{\mathcal{G}_{\varepsilon, \delta}}^{\text{KLD}}}\right) \quad (\text{A.5})$$

where $\theta_{\mathcal{G}_{\varepsilon, \delta}}^{\text{KLD}} := \text{argmin}_{\theta \in \Theta} \text{KLD}(\mathcal{G}_{\varepsilon, \delta} \| f_\theta)$ and $p(x | z_{1:m})$ is the Bayesian posterior predictive distribution (using ℓ_0) based on (synthetic) data $z_{1:m}$,

$$p(x | z_{1:m}) = \int f_\theta(x) \pi(\theta | z_{1:m}) d\theta \quad (\text{A.6})$$

Proof. Firstly fix the the divergence D between the KLD minimising model to $\mathcal{G}_{\varepsilon, \delta}$ and DGP F_0 as

$$K_\infty = D\left(F_0 \| f_{\theta_{\mathcal{G}_{\varepsilon, \delta}}^{\text{KLD}}}\right). \quad (\text{A.7})$$

Now either $\min_{\theta \in \Theta} D(F_0 \| f_\theta) = K_\infty$ also, in which case the D -minimising approximation to F_0 is the same distance from F_0 (in terms of distance D), as the KLD minimising approximation to $\mathcal{G}_{\varepsilon, \delta}$ and Eq. (A.5) hold with equality. Such a situation would happen if $\mathcal{G}_{\varepsilon, \delta} = F_0 = f(\cdot; \theta_0)$ for example. Or we can find π such that $\mathbb{E}_z [D(F_0 \| p(\cdot | z_{1:m}))] < K_\infty$, for example $\pi(\theta) = 1_{\theta'}$ for θ' such that $D(F_0 \| f(\cdot; \theta')) < K_\infty$ and therefore Eq. (A.5) holds with $m = 0$. \square

We know that under regularity conditions and as $m \rightarrow \infty$, Bayes rule will concentrate about the parameter $\theta_{\mathcal{G}_{\varepsilon, \delta}}^{\text{KLD}} := \text{argmin}_{\theta \in \Theta} \text{KLD}(\mathcal{G}_{\varepsilon, \delta} \| f(\cdot; \theta))$ (Berk et al., 1966); as such we can conclude that given an infinite sample

from an s-DGP $\mathcal{G}_{\varepsilon,\delta} \neq F_0$, it is not necessarily optimal to use all of the data available, contrary to the logic of standard statistical analyses.

Note that in general there is nothing about Proposition 1 that is specific about using traditional Bayesian updating and learning about $\theta_{\mathcal{G}_{\varepsilon,\delta}}^{\text{KLD}}$ in the limit. The proof of the proposition is unchanged if we consider for example general Bayesian updating using $\ell^{(\beta)}(x, f_\theta)$ and limiting parameter $\theta_{\mathcal{G}_{\varepsilon,\delta}}^{\beta\text{D}} := \operatorname{argmin}_{\theta \in \Theta} \beta\text{D}(\mathcal{G}_{\varepsilon,\delta} \| f(\cdot; \theta))$.

A.2.2 Proof of Proposition 2

Next we provide a result that ensures we do not waste synthetic data when \hat{m} is less than the maximum amount of synthetic data available. If more synthetic data is available than the \hat{m} that are used for inference (e.g. sampling $z_{1:m}, m \rightarrow \infty$ from a GAN), we can average the posterior predictive distribution across different realisations and improve the performance of the predictive distribution if we consider convex proper scoring rules such as the logarithmic score. The proof of this result is simple and relies on Jensen’s inequality.

Proposition 2 (Predictive Averaging). *Given divergence D with convex scoring rule, s , averaging over different realisations (formulated using different realisations of $z_{1:m}$ indicated by superscript (b)) of the posterior predictive depending on different synthetic data sets improves inference:*

$$\mathbb{E}_z D \left(F_0 \parallel \frac{1}{B} \sum_{b=1}^B \tilde{p} \left(x \mid z_{1:m}^{(b)} \right) \right) \leq \mathbb{E}_z D \left(F_0 \parallel \tilde{p} \left(x \mid z_{1:m}^{(b)} \right) \right).$$

Proof.

$$\begin{aligned} \mathbb{E}_z D \left(F_0 \parallel \frac{1}{B} \sum_{b=1}^B \tilde{p} \left(x \mid z_{1:m}^{(b)} \right) \right) &= \mathbb{E}_z \mathbb{E}_{x \sim f_0} \left[s \left(x, \frac{1}{B} \sum_{b=1}^B \tilde{p} \left(\cdot \mid z_{1:m}^{(b)} \right) \right) \right] - \mathbb{E}_z \mathbb{E}_{x \sim f_0} [s(x, f_0)] \\ &\leq \mathbb{E}_z \mathbb{E}_{x \sim f_0} \left[\frac{1}{B} \sum_{b=1}^B s \left(x, \tilde{p} \left(\cdot \mid z_{1:m}^{(b)} \right) \right) \right] - \mathbb{E}_z \mathbb{E}_{x \sim f_0} [s(x, f_0)] \end{aligned} \quad (\text{A.8})$$

$$\begin{aligned} &= \frac{1}{B} \sum_{b=1}^B \mathbb{E}_z \mathbb{E}_{x \sim f_0} \left[s \left(x, \tilde{p} \left(\cdot \mid z_{1:m}^{(b)} \right) \right) \right] - \mathbb{E}_z \mathbb{E}_{x \sim f_0} [s(x, f_0)] \quad (\text{A.9}) \\ &= \mathbb{E}_z \mathbb{E}_{x \sim f_0} [s(x, \tilde{p}(\cdot \mid z_{1:m}^{\hat{m}}))] - \mathbb{E}_z \mathbb{E}_{x \sim f_0} [s(x, f_0)] \\ &= \mathbb{E}_z D \left(F_0 \parallel \tilde{p} \left(x \mid z_{1:m}^{(b)} \right) \right) \end{aligned}$$

Where A.8 uses Jensen’s inequality and the convexity of s and A.9 uses the identical distribution of $\tilde{p}(x \mid z_{1:m}^{(b)})$ across varying b . □

The significance of this is that more synthetic data can always be used to improve the predictive distribution, but not by naïvely using all of it to learn at once.

A.2.3 Elaboration of Remark 1

Another way to obtain \hat{m} could be dependent on the concrete data stream through the consideration of the trajectory of the evaluation criteria for a concrete sequence of data items. This involves finding the minimum of:

$$\hat{m} := \operatorname{argmin}_{0 \leq m \leq M} \frac{1}{N} \sum_{j=1}^N s(x'_j, p^\ell(\cdot \mid z_{1:m}))$$

Finding this minimum in practice involves potentially adapting the upper bound via optimisation i.e. successively extending a search interval until the local minima is contained (see e.g. http://www.optimization-online.org/DB_FILE/2007/10/1801.pdf). This estimator depends on the order of the data; the performance of the resulting predictor can be improved using an analog of Proposition 2 by averaging across different shuffles.

A.3 The Differential Privacy for Synthetic Data generated under the Normal-Laplace mechanism

Here we formalise how the Laplace mechanism (Dwork et al., 2014) provides synthetic data with differential privacy guarantees.

Proposition 3 (Synthetic Data via the Laplace Mechanism). *Given real data $x_{1:n} \in D^n$, synthetic data, $z_{1:n} \in D^n$, generated according to the Laplace mechanism, $\mathcal{T}_{\mathcal{A}} : \mathbb{R}^n \rightarrow \mathbb{R}^n$ with $z_{1:n} = \mathcal{T}_{\mathcal{A}}(x_{1:n}) = x_{1:n} + \delta_{1:n}$ where $\delta_{1:n} \stackrel{\text{i.i.d.}}{\sim} \text{Laplace}(0, \lambda)$, is $(\varepsilon, 0)$ -differentially private with $\varepsilon = \max_{x_n, x'_n} \frac{|x_n - x'_n|}{\lambda}$.*

Proof. Fix $x_{1:n} \in D^n$ and consider $x'_{1:n} = \{x_{1:n-1}, x'_n\} \in D^n$

$$\begin{aligned} & \left| \ln \left(\frac{P(\mathcal{T}_{\mathcal{A}}(x_{1:n}) = z_{1:n})}{P(\mathcal{T}_{\mathcal{A}}(x'_{1:n}) = z_{1:n})} \right) \right| \\ &= \left| \ln \left(\frac{P(x_{1:n} + \delta_{1:n} = z_{1:n})}{P(x'_{1:n} + \delta_{1:n} = z_{1:n})} \right) \right| \\ &= \left| \ln \left(\frac{\frac{1}{(2\lambda)^n} \exp\left(-\frac{\sum_{i=1}^n |x_i - z_i|}{\lambda}\right)}{\frac{1}{(2\lambda)^n} \exp\left(-\frac{\sum_{i=1}^n |x'_i - z_i|}{\lambda}\right)} \right) \right| \\ &= \left| \frac{|x_n - z_n|}{\lambda} - \frac{|x'_n - z_n|}{\lambda} \right| \\ &\leq \frac{|x_n - x'_n|}{\lambda}, \end{aligned}$$

As a result, such a procedure provides differential privacy of $\varepsilon = \max_{x_n, x'_n} \frac{|x_n - x'_n|}{\lambda}$ by Definition 1 of Dwork et al. (2006) \square

In situations where $|x_n - x'_n|$ is unbounded, an artificial upper bound B can be imposed with corresponding truncation bounds $\{a, b\}$ with $b - a = B$. For example, this could take the form $\{a, b\} = \{\mu + \frac{B}{2}, \mu - \frac{B}{2}\}$ where μ is the mean of F_0 . Any observation $x_i \notin (a, b)$ is instead considered as $\tilde{x}_i = \arg \min_{y \in \{a, b\}} |y - x_i|$ before the addition of the Laplace noise δ_i . Unlike Bernstein and Sheldon (2018) we cannot simply redact observations outside the truncation bounds as this would change the dimension of the response and leak privacy. As a result, the truncated Laplace mechanism for unbounded real data is defined as $z_{1:n} = \mathcal{T}_{\mathcal{A}}(x_{1:n}) = \{\min(\max(a, x), b)\}_{1:n} + \delta_{1:n}$ with $\delta_{1:n} \stackrel{\text{i.i.d.}}{\sim} \text{Laplace}(0, \lambda)$ and provides $(\varepsilon, 0)$ -differential privacy with $\varepsilon = \frac{b-a}{\lambda}$.

We note here that the Laplace mechanism provides a more naïve and much simpler method for producing synthetic data compared with methods such as the DP-GAN (Xie et al., 2018) or PATE-GAN Jordon et al. (2018), and that clearly if estimation of variance is important then this mechanism constitutes a poor method to produce synthetic data. However, if one is interested in measures of central tendency, for example estimating coefficients for a regression model then the Laplace mechanism will preserve such features in expectation across the data, which is not necessarily guaranteed by the GAN based methods. This shows that different methods, producing the same differential privacy guarantee, can have differing desirability to Learner, L , depending on which aspects of the DGP L wishes to capture.

A.4 Motivating Schematic

Fig. A.3 provides a cartoon representing our interpretation of the learning trajectory in the space of distributions for data. Such an interpretation is substantiated by the experiments in Section 4 of the main paper and further in Section A.6.5. We consider two cases, one where the synthetic data is able to get inference closer to F_0 and one where synthetic data immediately makes things worse under traditional Bayesian updating because the beliefs prior to observing the synthetic data were sufficiently informative. Note that ‘distances’ on this schematic are according to the chosen divergence D .

The learner L starts at their prior predictive before observing any data, $p(x) = \int f_{\theta}(x)\pi(\theta)d\theta$, and uses their own data $x_{1:n_L}^L$ and Bayes rule (Eq. (6) from the main paper and $\ell_0(z, f_{\theta})$) to update their beliefs. Data $x_{1:n_L}^L \sim F_0$

is not privatised and thus using standard updating draws inference towards the DGP, F_0 . By Bayesian additivity this posterior, $\pi(\theta | x_{1:n_L}^L)$ given observations from F_0 becomes the prior for inference using observations $z_{1:m}$. We thus interpret any inference that L can do on their own data as providing a strongly informative prior about F_0 . Again, we stress that our framework allows for the possibility that $n_L = 0$ here. However, we show later that $n_L > 0$ offers an inferential ‘momentum’ in the direction of F_0 under the βD and allows for the synthetic data to bring inferences closer to F_0 on the learning trajectory than is possible under traditional Bayesian updating.

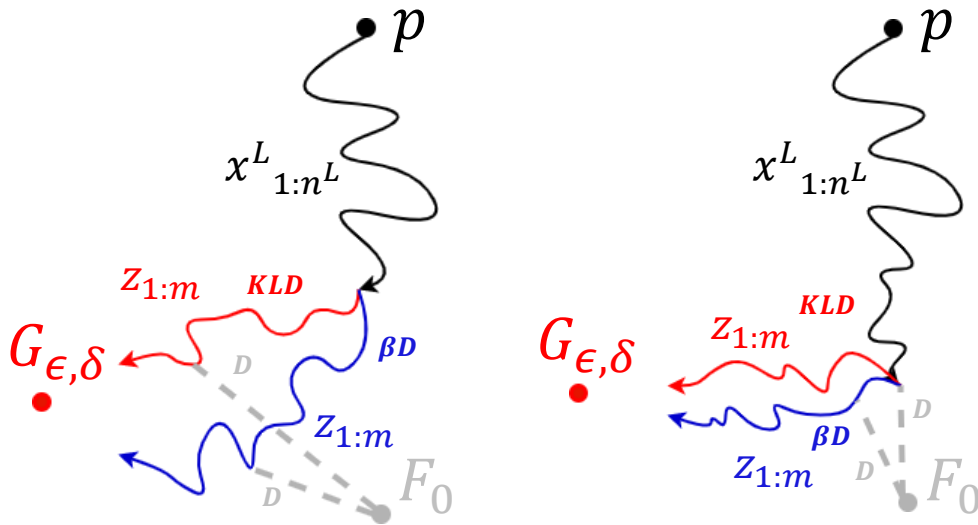


Figure A.3: The statistical geometry of learning using synthetic data: Starting from prior predictive (p), updating using $x_{1:n_L}^L \sim F_0$ takes inference towards F_0 , before $z_{1:m} \sim \mathcal{G}_{\epsilon, \delta}$ takes inference towards $\mathcal{G}_{\epsilon, \delta}$ as $m \rightarrow \infty$. **Red** is traditional Bayesian updating (using $\ell_0(z, f_\theta)$) and **blue** is general Bayesian updating using $\ell^{(\beta)}(z, f_\theta)$. Distances are defined by the divergence D . Left: Fewer n_L mean that both learning methods are able to use synthetic data to improve inference for F_0 according to D . Right: Greater n_L means that before using synthetic data L is closer to F_0 ; when adding synthetic data here traditional Bayesian updating immediately takes inference away from F_0 with respect to D .

After the initial steps towards F_0 following the use of $x_{1:n_L}^L$, L starts learning from the synthetic data $z_{1:m}$ and therefore inference begins to move towards $\mathcal{G}_{\epsilon, \delta}$. We argue that this does not imply inference is necessarily getting farther from F_0 providing acceptance of our minimal assumption that $\mathcal{G}_{\epsilon, \delta}$ captures some useful information about F_0 , i.e. we assume that in the model space defined by D , $\mathcal{G}_{\epsilon, \delta}$ and F_0 are proximal. Such a phenomenon is depicted on the left-hand side of Fig. A.3: the red line corresponds to using Bayes’ rule when updating using the synthetic data, and we indicate a point on this trajectory that is closer to F_0 (according to the chosen divergence D) than the inference using only $x_{1:n}$. Up until this point learning about $\mathcal{G}_{\epsilon, \delta}$ was also helping to learn about F_0 but after such a point inference begins to be pulled away from F_0 . However, on the right-hand side of Figure A.3 we acknowledge that this is not always the case, there can be situations where synthetic data immediately takes inference away from F_0 . This will happen if the prior information (including the learner’s own data) is very strong, or if the s-DGP is far from F_0 .

Additionally, in blue we plot an example trajectory for learning using the βD . We argue that the βD has the ability to get closer to F_0 because of its robustness properties. The examples in Section A.1.1 have demonstrated that inference using the βD , unlike traditional Bayesian inference, is able to ignore outliers while still learning from inlying observations. As a result, initially the βD inference is able to learn from observations from the s-DGP that support the inference based on $x_{1:n_L}^L$ and dynamically downweight those that do not, therefore getting closer to F_0 . Conversely, traditional Bayesian inference is influenced more by observations that disagree with F_0 and thus gets pulled more quickly towards $\mathcal{G}_{\epsilon, \delta}$. This further reinforces the benefits that can be gained by beginning analysis using real data to impart some ‘momentum’ towards F_0 when learning from synthetic samples under the βD .

A.5 Prescribed Methodology

The discussion surrounding learning trajectories has demonstrated that a promising way to improve inference using synthetic data is to use the β_D -loss combined with a reduced number of synthetic data items. A resulting question is how can one actually action such a procedure for inference given a realisation $z_{1:M} \sim \mathcal{G}_{\varepsilon,\delta}$, for $0 < M \leq \infty$ and independent testing set $x'_{1:N} \sim F_0$, for $0 < N \leq \infty$. To answer this we must address the following questions.

1. How exactly can realisations of real and synthetic datasets be used to estimate \hat{m} ?
2. Given that we estimate $\hat{m} < M$, which \hat{m} data items out of the M available should we use for inference?

We provide answers to these two questions in the next subsections.

A.5.1 Finding \hat{m}

The optimal m^* as defined in Eq. (12) of the main paper is an expectation over synthetic data $z \sim \mathcal{G}_{\varepsilon,\delta}$ and real data from the DGP, $x \sim F_0$, where the second expectation is hidden inside the definition of the Divergence (Definition 2). Given that, at best, we have a sample from the DGP, $x'_{1:N} \sim F_0$, and a sample from s-DGP $z_{1:M} \sim \mathcal{G}_{\varepsilon,\delta}$, m^* can be estimated by \hat{m} as defined in Eq. (13) of the main paper. We note that even in the case where the s-DGP density could be given to the learner L , the expectation in Eq. (12) would likely be intractable and sampling would be required to estimate this integral regardless.

In the case where L is given the ability to sample from the s-DGP arbitrarily, they can continue to sample independently from $\mathcal{G}_{\varepsilon,\delta}$ to calculate \hat{m} . Clearly the more samples that they draw, the more accurate this estimation will be, but in reality fixing a computational sampling budget within this scheme is both inevitable and sensible.

When this is not the case, namely there exists $z_{1:M} \sim \mathcal{G}_{\varepsilon,\delta}$, for $0 < M < \infty$, the learner can repeatedly sample with or without replacement from $z_{1:M}$ to estimate \hat{m} . Clearly repeated sampling is only beneficial to the extent to which new samples are not too dependent on previous ones, something that will be determined by the relative size of the m 's under consideration compared with M . If $\hat{m} \approx M$ (i.e. m is of the same order of magnitude as M) then estimating this integral from one sample is the best that the learner can do.

A.5.1.1 A p -value for the Use of Synthetic Data

In order to guard against the possible variance in calculating \hat{m} from collections of real and synthetic data that might not be sufficiently large, we wish to provide a minimum guarantee that inference using \hat{m} synthetic data samples is no worse than inference using only prior $\tilde{\pi}$ (including any of their own data and expert knowledge). In order to do so, the testing set $x'_{1:N} \sim F_0$ can be split into independent subsets, one of which is used to estimate \hat{m} using Eq. (12) of the paper, whilst the other subset is used to construct a p -value that the divergence D is significantly reduced using \hat{m} synthetic data samples compared to using no synthetic data at all, i.e. $m = 0$. The divergences are estimates as sums and therefore the central limit theorem can be invoked to construct such a p -value

Moreover, to guard against the variance in splitting a possible small testing set, this procedure can be repeated. For example, repeatedly splitting the data K times allows for the production of K p -values. Then a similar procedure to that considered in Watson and Holmes (2020) can be used to ‘aggregate’ these K p -values. They adapt a procedure of Meinshausen et al. (2009) which given a set of K p -values $\{p_1, \dots, p_K\}$ produces valid aggregated p -value,

$$p_{\text{aggregated}}^{(\text{median})} := \min(1, \text{Median}(2p_1, \dots, 2p_K)). \quad (\text{A.10})$$

This facilitates a valid and robust test for whether to use synthetic data or not.

- If this test fails to reject the null hypothesis then the synthetic data from $\mathcal{G}_{\varepsilon,\delta}$ is disregarded ($\hat{m} = 0$) and the learner should just continue with $\tilde{\pi}$.
- If this test rejects the null hypothesis in favour of using synthetic data then \hat{m} can be re-estimated using the whole testing set $x'_{1:N}$ and returned to the learner.

A.5.2 Inference Given \hat{m}

Given that L has estimated $\hat{m} < M$, how should they do inference using only \hat{m} out of a possible M samples? Should they simply take the first \hat{m} samples? This would introduce an undesirable dependence on the ordering of the data. Whilst this could be remedied by shuffling the data, we invoke Proposition 2 which shows that inference is improved by averaging posterior predictives over many synthetic data sets, $z_{1:\hat{m}}$ of size \hat{m} . By Proposition 2 the learner should repeatedly sample subsets of size \hat{m} from the M available, with or without replacement, conduct posterior inferences using each one independently, and then average their posterior predictions. This has been shown to perform better in expectation according to divergence D than using any single synthetic data subset of size \hat{m} .

A.6 Additional Experimental Details and Results

This section details all of the information referred to in Section 4 of the main paper; it provides explicit model definitions, explicit grids that were explored to produce the plots included in the paper, further plots to these experiments, and other information regarding the reproduction of the code including reference to our GitHub repository etc.

A.6.1 Explicit Loss Function Formulations

In the two sections below, we formally define the models that were used in the experiments discussed in the main paper; the parameters that we searched across are formally introduced here as well, to be followed with a full experimental grid.

A.6.1.1 Simulated Gaussian

For the simulated Gaussian experiments, the first loss function is given by the standard log-likelihood for the posterior when learning the parameters of a Gaussian distribution, $f_\theta(x) = \mathcal{N}(x; \mu, \sigma^2)$. It can be written as below, with the addition of a w parameter to indicate that this loss function also encompasses the reweighting approach mentioned in Section 3.2:

$$\ell_w(x_i; \theta) = -w \cdot \log f(x_i; \theta) \tag{A.11}$$

Our second loss function leverages the βD in lieu of standard Bayesian updating (and its connection to the KLD) and can be written in closed form:

$$\ell_\beta(x_i, f(x_i; \theta)) = -w_\beta \left(\frac{1}{\beta} f(x_i; \theta)^\beta - \frac{1}{\beta + 1} \int f(z; \theta)^{\beta+1} dz \right) = -w_\beta \left(\frac{1}{\beta} f(x_i; \theta)^\beta - \left((2\pi)^{\frac{\beta}{2}} (1 + \beta)^{\frac{3}{2}} \sigma^\beta \right)^{-1} \right), \tag{A.12}$$

where w_β is a ‘calibration weight’ (Bissiri et al., 2016), calculated via β and the data, that upweights the loss function to account for the ‘cautiousness’ of the βD . By this we mean that the βD -loss is generally smaller than the log-loss everywhere, rather than only in outlying regions of the data space.

In the case of these simulated examples we can also define a model (and associated log-loss function) that captures the noise-induced privatisation via the Laplace mechanism through the density of a Normal-Laplace convolution, which was first defined in (Reed, 2006), later corrected in (Amini and Rabbani, 2017) and now reformulated for our specific case of centred Laplace noise below:

$$\begin{aligned} \ell_{\text{Noise-Aware}}(x_i; \mu, \sigma, \lambda) = \\ - \log \left(\frac{1}{4\lambda} \left(e^{\frac{\mu-y}{\lambda} + \frac{\sigma^2}{2\lambda^2}} \left(1 + \operatorname{erf} \left(\frac{y-\mu}{\sigma\sqrt{2}} - \frac{\sigma}{\lambda\sqrt{2}} \right) \right) + e^{\frac{y-\mu}{\lambda} + \frac{\sigma^2}{2\lambda^2}} \left(1 - \operatorname{erf} \left(\frac{y-\mu}{\sigma\sqrt{2}} + \frac{\sigma}{\lambda\sqrt{2}} \right) \right) \right) \right) \end{aligned} \tag{A.13}$$

A.6.1.2 Logistic Regression

In the case of our logistic regression examples on real-world datasets, w again allows us to reweight the standard log-likelihood for robustness when learning on the synthetic data to formulate our first loss function based on the

logit-parameterised Bernoulli density function:

$$\ell_w(x_i; y_i, \alpha, \theta) = -w \cdot \log \left(\text{logistic}(\alpha + x_i \cdot \theta)^{y_i} + (1 - \text{logistic}(\alpha + x_i \cdot \theta))^{(1-y_i)} \right), \quad (\text{A.14})$$

where:

$$\text{logistic}(x) = \frac{1}{1 + e^{-x}}. \quad (\text{A.15})$$

Applying the β D-loss to the same logit-parameterised Bernoulli density function becomes our second loss function:

$$\begin{aligned} \ell_\beta(x_i; y_i, \alpha, \theta) = & -w_\beta \left(\frac{1}{\beta} \left(\text{logistic}(\alpha + x_i \cdot \theta)^{y_i} + (1 - \text{logistic}(\alpha + x_i \cdot \theta))^{(1-y_i)} \right)^\beta + \right. \\ & \left. \frac{1}{\beta + 1} \left(\text{logistic}(\alpha + x_i \cdot \theta)^{\beta+1} + (1 - \text{logistic}(\alpha + x_i \cdot \theta))^{\beta+1} \right) \right) \end{aligned} \quad (\text{A.16})$$

Here, we cannot formulate a ‘noise-aware’ counterpart as the privatisation is via the black-box generations of the PATE-GAN.

A.6.2 Evaluation Criteria

Here we explicitly define each of our evaluation criteria, which are in general calculated via an evaluation set and an approximation to the posterior predictive using the samples drawn from MCMC chains. For these definitions, we let P and Q be two probability measures.

A.6.2.1 KLD

The KLD is defined as:

$$D_{\text{KL}}(P \parallel Q) = \int_{\mathcal{X}} \log \left(\frac{dP}{dQ} \right) dP$$

A.6.2.2 Log Score

The log score as in Gneiting and Raftery (2007) is a special case of a proper scoring rule defined as:

$$\mathbb{E}_{\theta \sim \pi(\theta | x_{1:n})} [\log f(z; \theta)] \quad (\text{A.17})$$

A.6.2.3 Wasserstein Distance

Following Rueschendorff (1977) we define the Wasserstein distance as:

$$D_W(P, Q) = \sup \left(\int f dP - \int f dQ \mid \text{Lipschitz}(f) \leq 1 \right).$$

Where $\text{Lipschitz}(f) = \sup_{x \neq y} \frac{|f(x) - f(y)|}{\|x - y\|}$

A.6.2.4 AUROC

For a probabilistic binary classification algorithm, the receiver operating characteristic (ROC) curve plots the true positive rate against the false positive rate as a parametric plot across different threshold settings. The area under this curve (AUROC) is equal to the probability that a classifier will rank some random positively labelled datapoint higher than a randomly chosen negatively labelled one; it comprises a common means of evaluating the performance of such classifiers.

$$A = \int_{x=0}^1 \text{TPR}(\text{FPR}^{-1}(x)) dx$$

where $\text{FPR}^{-1}(x)$ is the pseudo-inverse of the FPR that maps a false positive rate of x to the corresponding choice of threshold. Following Calders and Jaroszewicz (2007) it can also be estimated via:

$$\frac{\sum_{t_0 \in \mathcal{D}^0} \sum_{t_1 \in \mathcal{D}^1} \mathbf{1}[f(t_0) < f(t_1)]}{|\mathcal{D}^0| \cdot |\mathcal{D}^1|}$$

A.6.3 Reproducing Our Experiments

In order to reproduce the results shown in this supplement and in the main paper, one must execute large scale experiments to explore the effect of various parameters across large grids. This amounts to a significant computational workload that was facilitated by recent advances in probabilistic programming in Julia’s Turing PPL (Ge et al., 2018), MLJ (Blaom et al., 2020) and Stan (Carpenter et al., 2017) and the use of large compute nodes. Specifically, we predominantly relied upon a SLURM cluster managed by XXXXX.

All of the code, experimental configuration specifications and other requirements are laid out in our GitHub repository¹; below are the parameter ranges and other values used to produce the plots in the case of the two experiment types discussed in the paper:

- 6000 MCMC samples were taken per chain in the case of logistic regression; 4000 in the case of the Gaussian simulations. In both cases, 500 warm-up samples were sampled and subsequently discarded.
- We used Stan’s NUTS (Hoffman and Gelman, 2014) sampler and the NUTS sampler provided by Turing to carry out the majority of the inference tasks; we monitored \hat{R} and other convergence criteria when designing the experiments and during their execution to ensure consistent convergence.
- For the $\beta\mathcal{D}$ based models, $\beta \in \{0.1, 0.2, 0.25, 0.4, 0.5, 0.6, 0.75, 0.8, 0.9\}$. We also upweight each posterior using a multiplicative $w_\beta = 1.25$ to account for the fact that the $\beta\mathcal{D}$ is more ‘cautious’ in general than standard updating.
- For the standard reweighted models, $w \in \{0.0, 0.25, 0.5, 0.75, 1.0\}$.
- Data quantities:
 - For the simulated Gaussian experiment we jointly varied n and m with $n \in \{2, 4, 6, 8, 10, 13, 16, 19, 22, 25, 30, 35, 40, 50, 75, 100\}$ and $m \in \{1, 2, \dots, 99, 100, 120, 140, 160, 180, 200\}$.
 - For logistic regression we traversed a grid of proportional quantities of data rather than explicit n ’s for ease of comparison across the chosen datasets, $\alpha_{\text{real}} \in \{0.025, 0.05, 0.1, 0.25, 0.5, 1.0\}$ and $\alpha_{\text{synth}} \in \{0.0, 0.01, 0.02, 0.03, 0.04, 0.05, 0.075, 0.1, 0.15, 0.2, 0.4, 0.6, 1.0\}$.

Note that in both cases, we also ran a consecutive stream of real data values without any synthetic data to produce the black lines plotted on the branching plots and to give a means of comparing the performance of synthetic data, through the expected minima (or maxima in the case of AUROC), with the best case scenario of more real data allowing us to calculate the approximate effective number of real samples that the synthetic data could provide (see the following Section A.6.4).

- For evaluation, we generated an additional 500 samples from F_0 for the Gaussian, and utilised 5-fold cross validation for the logistic regressions where one fold was used for evaluation in each of the five steps.
- Priors:
 - In the case of our Gaussian model, we placed conjugate priors on θ with $\sigma^2 \sim \text{InverseGamma}(\alpha_p, \beta_p)$ and $\mu \sim \mathcal{N}(\mu_p, \sigma_p * \sigma)$. Here we set $\alpha_p = 2.0, \beta_p = 4.0, \mu_p \in \{0.0, 1.0, 3.0\}, \sigma_p \in \{1, 10, 30\}$.
 - We used uninformative Gaussian priors for the logistic regressions’ α (the intercept) and θ (other parameters), e.g. $\alpha, \theta \sim \mathcal{N}(0, 50)$
- For the logistic regression models, we initialised α and θ through 3 varying approaches:
 1. Using MLJ’s `LinearRegression` model to calculate the MLE given the step’s amount of real data n .

¹https://github.com/****

-
2. Setting θ to be a vector of 0's matching the dimension of the dataset
 3. Randomly initialising θ within a locality of 0 using a standard Gaussian model.

It is worth noting that this initialisation was not seen to have much observable effect in terms of MCMC convergence; the number of samples were carefully chosen alongside very effect sampling schemes such as NUTS and HMC to ensure convergence in almost all cases, even with very little or noisy data.

- We repeated all of the configurations defined by combinations of the parameter values specified above at least 100 times to ensure reasonable certainty in our results in the presence of multiple sources of noise (data generation, privatisation and MCMC). During each of these 'full iterations' we specified and recorded a randomised seed to ensure that the real data used was reshuffled or different each time for the logistic regression and simulated Gaussian experiments respectively. This then allows us to calculate expected curves across different realisations of varying amounts of real data.

A.6.3.1 Datasets Used for Logistic Regression

The Framingham Cohort Dataset contains 4240 rows and 15 predictors, a mix of binary labels and continuous or discrete numerics. The label is a binary indicator for someone's ten year risk of coronary heart disease. Many of the columns such as age, education, cigarettes smoked per day and more pose genuine privacy concerns to the subjects of this dataset.

The UCI Heart Dataset contains 303 rows and 14 predictors, again a mix of binary labels and continuous or discrete numerics. The label is a binary indicator for the presence of heart disease in a subject. Many of the attributes pose genuine privacy concerns to the subjects of this dataset.

A.6.4 Elaboration on the Formulation and Meaning of the Figures

The following section further details how each type of figure shown in the paper is made, and how they should be interpreted:

- **The 'branching' plots** (as in Figures A.6, A.7, A.8, A.9, A.10, A.11, A.12, A.13, A.14, A.15 and Figure 1 of the main paper (and Figure 4 which is a special case)) show the total amounts of data on the x axis used to train various model via MCMC, each model corresponding to a single point on the plot. This amount is totalled in the sense that it corresponds to some amount of real data n_L added on to some amount of synthetic data m . Each 'branch' of these plots fixes the amount of real data it represents at the root of its branch from the black line which represents a varying amount of real data and no synthetic samples. Each branch is then colour coded and corresponds to some fixed quantity of real data n_L plus a varying amount of synthetic data, such that the amount of synthetic samples included in learning up to a point on the x axis can be calculated by subtracting the fixed real data quantity n_L from the x axis value. The y axis is relatively clear in corresponding to the relevant criteria value when the model trained at each point of the branching curves is evaluated. Note that these plots directly show the 'learning trajectory' as depicted in Figure A.3
- **The model comparison plots** (as in Figures A.16, A.17, A.18, A.19, A.20, A.21, A.22, A.23, A.24, A.25 and Figure 3 of the main paper) are in some ways just a more specific view of the 'branching' plots discussed above, in that they fix the real amount of data to some n_L and simply illustrate the performance of the models under varying synthetic data quantity m alongside one another. This is essentially a layering of a single consistent branch from each 'branching' plot layered on top of each other across all of the model configurations of interest.
- **The n -effective plots** (as in Figures A.26, A.27, A.28 and Figure 2 of the main paper) illustrate the maximal effective number of real samples that can be gained through the use of synthetic data under varying real data quantity n_L . In order to illustrate this, we calculate bootstrapped (Efron and Tibshirani, 1994) mean and variance of the minima / maxima by first taking the expectation over each seed / iteration / realisation of a curve alongside the synthetic data varying; this is done separately for each 'branch' (i.e. fixed real data quantity n_L) to get an expected curve for each. The turning point of these curves is then matched with the closest realised point along the black line representing varying amounts of real data without any synthetic data in order to produce an estimate for the amount of real data samples this turning point

effectively corresponds to. Namely, the additional number of real samples required to achieve the same minimum / maximum criteria value when learning using the optimal amount of synthetic data.

This process is done in the bootstrap paradigm such that we repeatedly sample $N = 100$ seeds / iterations / curves from those collected during the full experiment, the turning point corresponding to this expectation over N curves is then calculated; this is repeated $B = 200$ times to then calculate a bootstrapped mean and variance for the best (i.e. at the turning point in synthetic data) effective number of real samples for each amount of fixed real data.

This can be expressed as below, by taking an evaluation set $x'_{1:n'} \sim F_0$ and then by calculating B $n_{\text{eff}}^{(b)}$ s for each real data quantity n_L that we take, alongside varying synthetic samples. Each $n_{\text{eff}}^{(b)}$ is a bootstrap n -effective sample formulated using the the minimum of the expected curve arising across a randomly sampled $N = 100$ seeds / iterations / curves that is then ‘matched’ with a similar expected curve arising from $R = 100$ sampled real-only (black lines) seeds / iterations / curves to provide an estimation for the number of real samples each minimum represents:

$$n_{\text{eff}}^{(b)} = \operatorname{argmin}_t \left| \frac{1}{M} \sum_{j=1}^M s(x', p(\cdot | x_{1:n_L+t}^{(j)})) - \min_m \frac{1}{N} \sum_{i=1}^N s(x', \tilde{p}(\cdot | x_{1:n_L}^{(i)} z_{1:m}^{(i)})) \right|$$

This gives rise to a collection of B bootstrap samples for each value of n_L from which we can compute a bootstrapped mean and variance to present in our n -effective plots.

A.6.5 Further Results and Figures

Figure A.4 shows the relationship between privacy and model misspecification in terms of the KLD. We observe that initially, using a small amount of synthetic data is preferable due to the amount of noise a small ε introduces; there is then a cross over point around $\varepsilon = 1$ to $\varepsilon = 10$ where using more data becomes more desirable as the level of noise decreases, until eventually at $\varepsilon = 100$ we see comparable performance from using the synthetic data to using the same amount of real data. This pattern of usefulness is slightly more complex in the case of a GAN based model as the usefulness of the data also relies on the convergence of the GAN and the overall representativeness of its generated samples through the effectiveness of training, regardless of the value of ε .

We can conduct a more fundamental investigation of the PATE-GAN’s behaviour under varying ε by observing through Figure A.5 the average predictor standard deviation in the resulting datasets generated by the GAN under different ε specifications. This allows us to observe the ‘mode collapse’ of the generative model when ε is sufficiently small and privacy is sufficiently high. Interestingly, as observed in Figure 4 from the main paper, this data is still somewhat useful, at least in small quantities, in learning about F_0 .

A.6.5.1 Branching Plots

Figures A.6, A.7, A.8, A.9, A.10, A.11, A.12, A.13, A.14, A.15 show the full suite of branching plots for all of our experiments. In each of these plots we investigate different privatisation levels and criteria of interest; we then draw comparisons amongst the model configurations. In particular we see the finite and asymptotic effectiveness of the β D across a wide range of β when compared to a range of standard and reweighted approaches. The ‘Noise-Aware’ models perform the best as is expected as these models are aware of the privatisation process and thus can go some way towards modelling it. In terms of KLD especially, we can see this asymptotic effectiveness via the black dashed line representing $\text{KLD}(F_0 \| f_{\theta^*})$ for $\theta^* = \theta_{\mathcal{G}_{\varepsilon,\delta}}^{\text{KLD}}$ in the case of models involving w and $\theta^* = \theta_{\mathcal{G}_{\varepsilon,\delta}}^{\beta\text{D}}$ for models involving β . These quantities represent the approximation to F_0 given an infinite sample from $\mathcal{G}_{\varepsilon,\delta}$ under the two model types. It can be seen that a relatively small increase in noise / privatisation in the Gaussian experiments can quite drastically change the effectiveness of using synthetic data, such that only when very little real data is available should its use be considered at all. For the logistic regression experiment datasets, we actually see a reduction in performance when using the β D on the UCI Heart dataset. This is likely due to the β D’s natural tendency to downweight samples, as upon inspection it appears that the two model families will converge to roughly similar criterion values.

A.6.5.2 Model Comparison Plots

Figures A.16, A.17, A.18, A.19, A.20, A.21, A.22, A.23, A.24, A.25 show the full suite of model comparison plots for all of our experiments. These plots allow us to directly compare the performance of different model configurations given an identical amount of real data n_L and an accompanying, varying amount of synthetic data. We can compare the most desirable \hat{m} values achieved by all of the models to observe that again, other than in the case of the UCI Heart dataset, the βD consistently performs well in comparison to other approaches. The models where w is set to 0 offer a baseline of sorts, with the points where each other model’s curve crosses its straight line representing when the various other model configurations stop being justifiable and synthetic data should not be used at all. It can be seen that not only does the βD achieve more desirable performance in the majority of cases, but it also remains robust to large amounts of synthetic data where other approaches fail to be effective and quickly lose out through the use of synthetic data. We offer all of these plots on fixed axes across each grid so that a reader can notice the narrowing scope and magnitude to which synthetic data is useful as more real data samples become available; this highlights the advantages of the βD in that it is a ‘safer’ option even in the situations where synthetic data cannot help the inference much in that it is more robust to the damage it can cause, especially when a user may not be able to calculate \hat{m} explicitly.

A.6.5.3 n -Effective Plots

Figures A.26, A.27, A.28 show the full suite of n -effective plots for all of our experiments, other than for the Framingham dataset which is already included in the main text. In these plots we observe some interesting phenomena, primarily in that the number of real effective samples to gain through synthetic data is related to the amount of real data that has already been used; in general we observe asymptotic behaviour in the criteria as the amount of real data increases meaning variation in the performance of synthetic data and the resulting turning points can indicate a greater amount of effective samples gained despite the actual criterion value improvement being marginal. As such, reading the x axis is in some ways misleading in that effective samples often ‘mean more’ in the sense that they indicate a greater improvement in the criteria under a smaller total amount of data. Again, we see that in the case of the UCI Heart dataset, the improvements offered by the βD are less significant and in some cases non-existent over standard approaches.

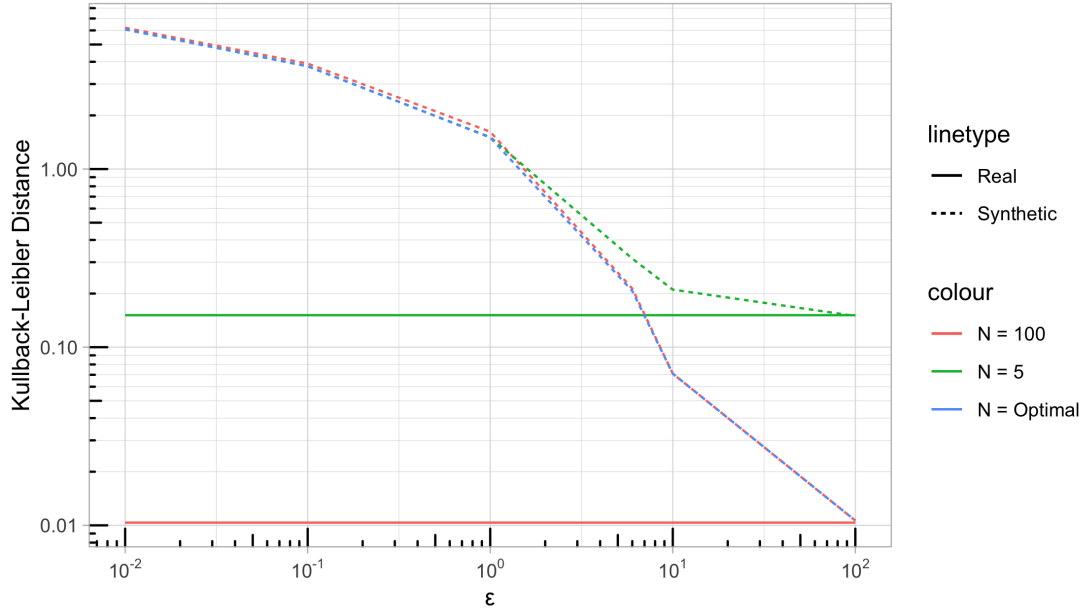


Figure A.4: This plot shows the average KLD between F_0 and the models arising from the specified amounts of real or synthetic data under varying DP-guarantees, the line types distinguish between real and synthetic, and colour indicates the data quantity used for learning. Here ‘optimal’ indicates that \hat{m} samples are used under each ϵ . As $\epsilon \rightarrow \infty$ the synthetic data becomes arbitrarily close to samples from F_0 through the Laplace mechanism such that the question of whether to use any or all of the synthetic data is most interesting at lower ϵ^2 .

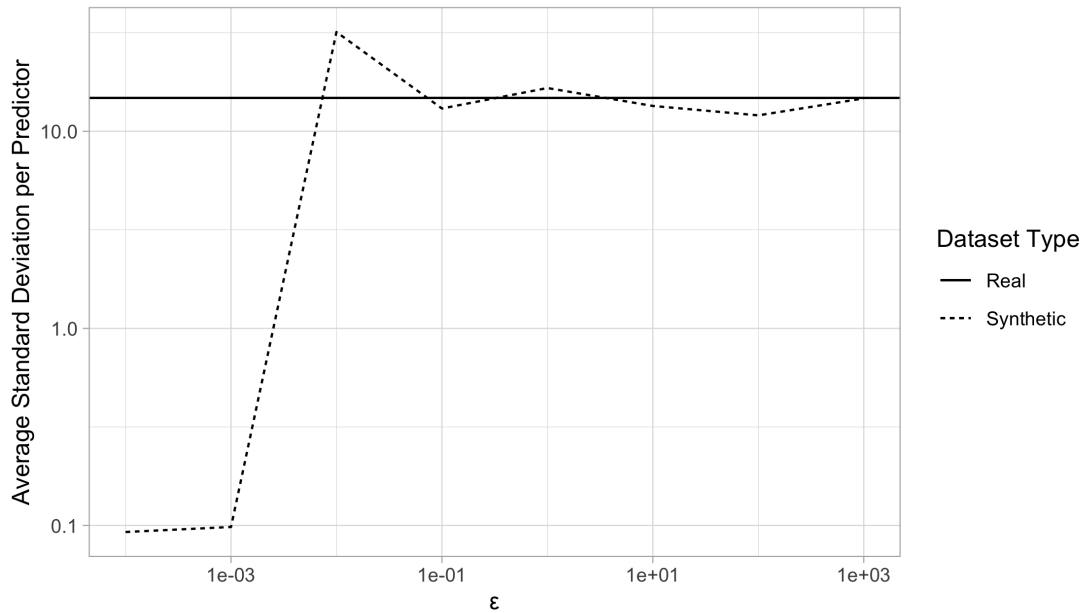


Figure A.5: Here, we present the averaged predictor standard deviation for datasets arising from various ϵ values. Similarly to Figure A.4, as $\epsilon \rightarrow \infty$ the synthetic data should more closely resemble the real dataset that was used to train it, plus whatever complications arise by nature of this training. It can be seen that as privacy increases with $\epsilon \rightarrow 0$ that there is a point $\epsilon^* \in [10^{-3}, 10^{-2}]$ where the predictors’ standard deviation collapses.

²Note that this is not consistently the case for GAN based methods as the utility of synthetic data is also limited by how well the GAN can initially capture F_0 from its training data regardless of the chosen ϵ .

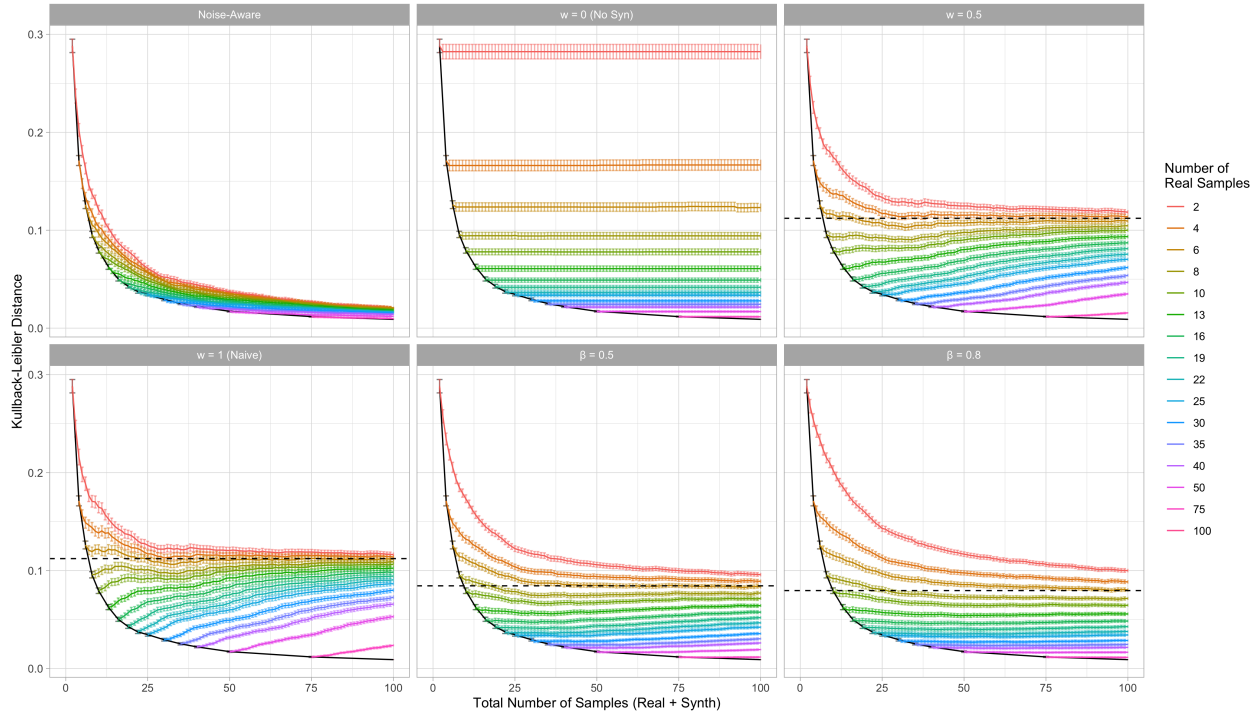


Figure A.6: Branching plots for each model configuration in the case of the simulated Gaussian experiments illustrating the KLD against the total number of samples where DP of $\epsilon = 8$ is achieved by the Laplace mechanism via noise of scale $\lambda = 0.75$.

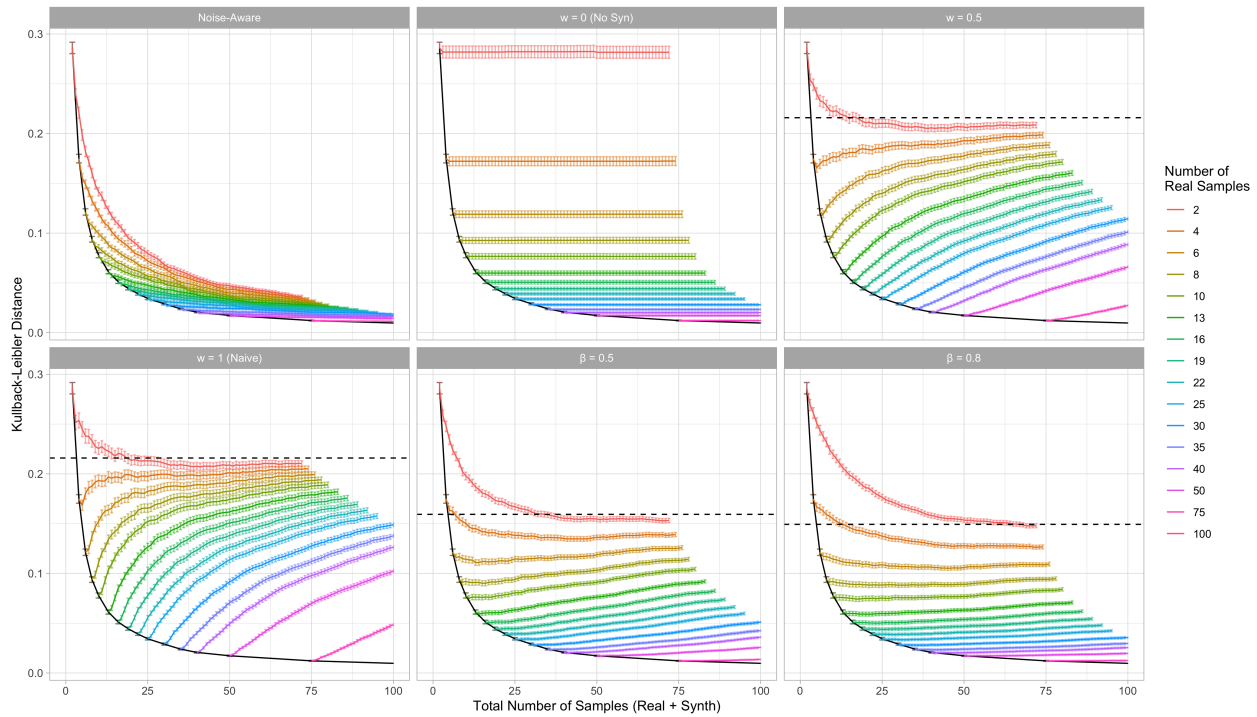


Figure A.7: Branching plots for each model configuration in the case of the simulated Gaussian experiments illustrating the KLD against the total number of samples where DP of $\epsilon = 6$ is achieved by the Laplace mechanism via noise of scale $\lambda = 1.0$.

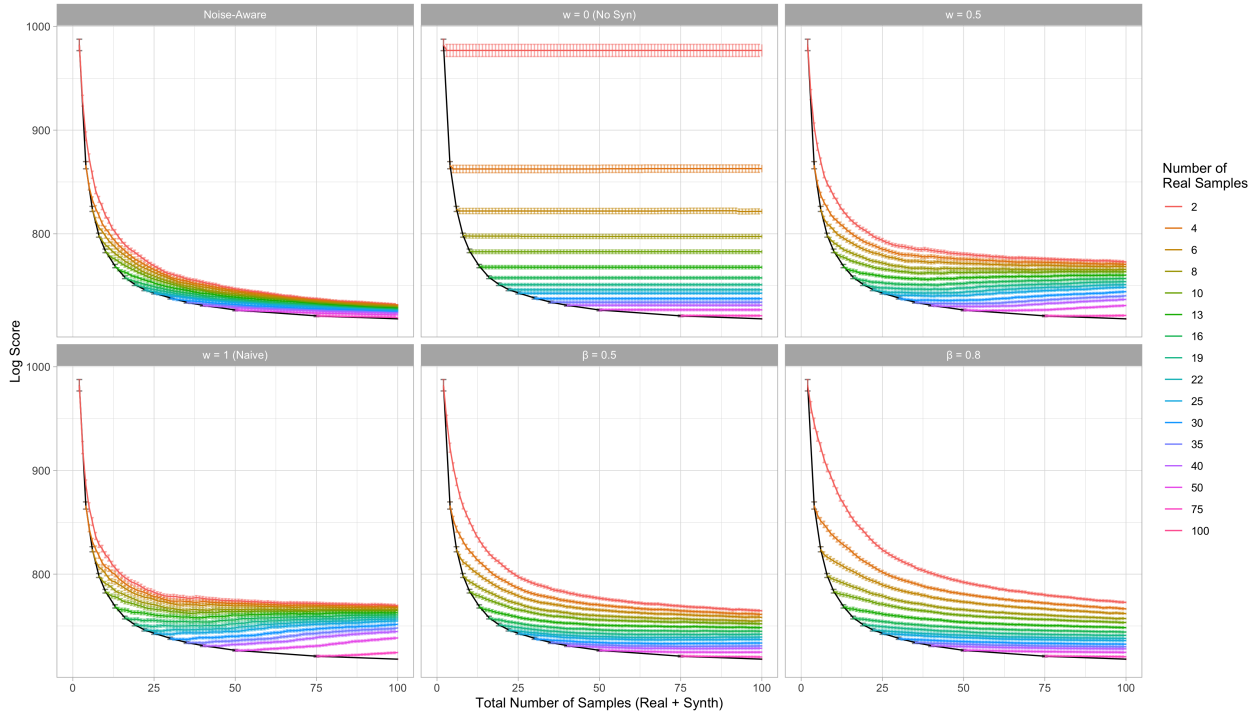


Figure A.8: Branching plots for each model configuration in the case of the simulated Gaussian experiments illustrating the log score against the total number of samples where DP of $\varepsilon = 8$ is achieved by the Laplace mechanism via noise of scale $\lambda = 0.75$.

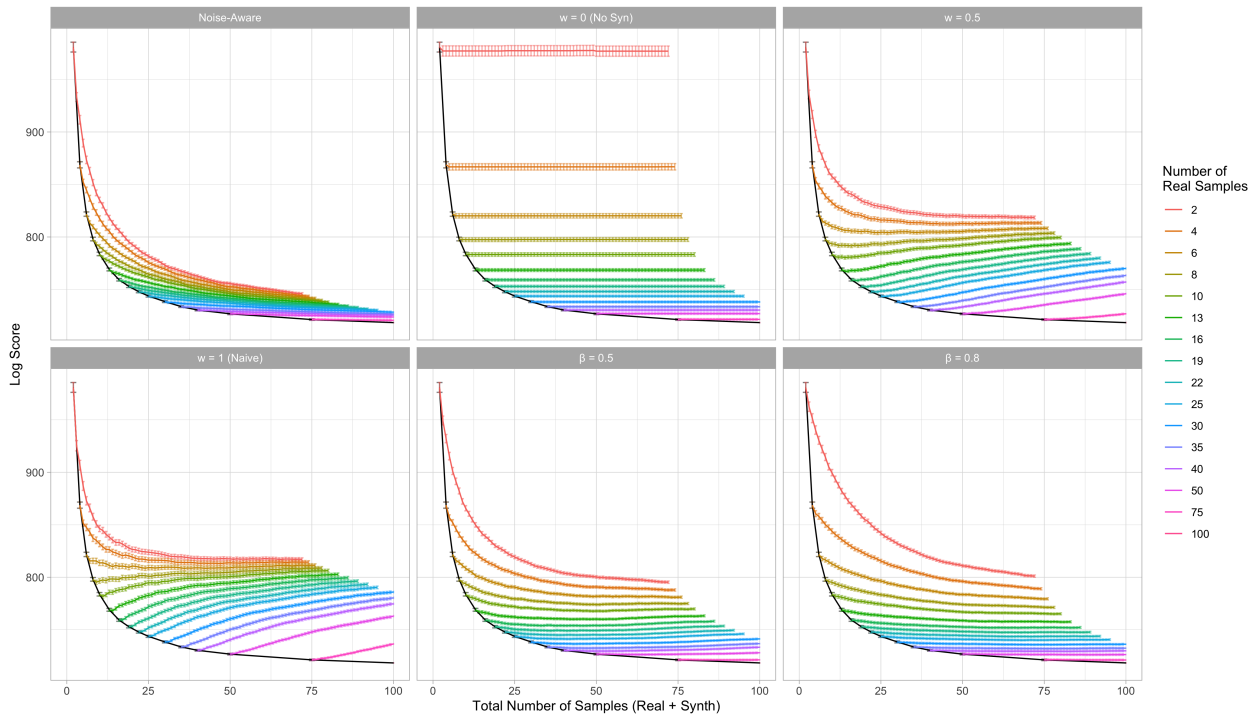


Figure A.9: Branching plots for each model configuration in the case of the simulated Gaussian experiments illustrating the log score against the total number of samples where DP of $\varepsilon = 6$ is achieved by the Laplace mechanism via noise of scale $\lambda = 1.0$.

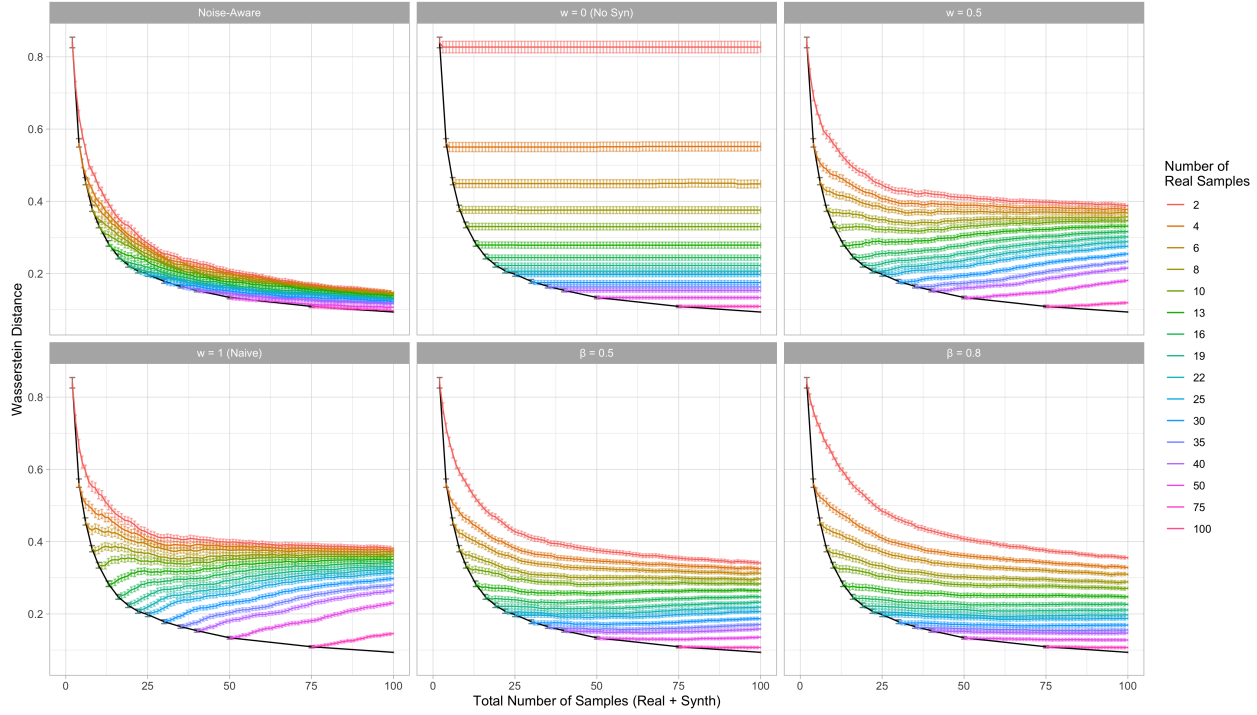


Figure A.10: Branching plots for each model configuration in the case of the simulated Gaussian experiments illustrating the Wasserstein distance against the total number of samples where DP of $\epsilon = 8$ is achieved by the Laplace mechanism via noise of scale $\lambda = 0.75$.

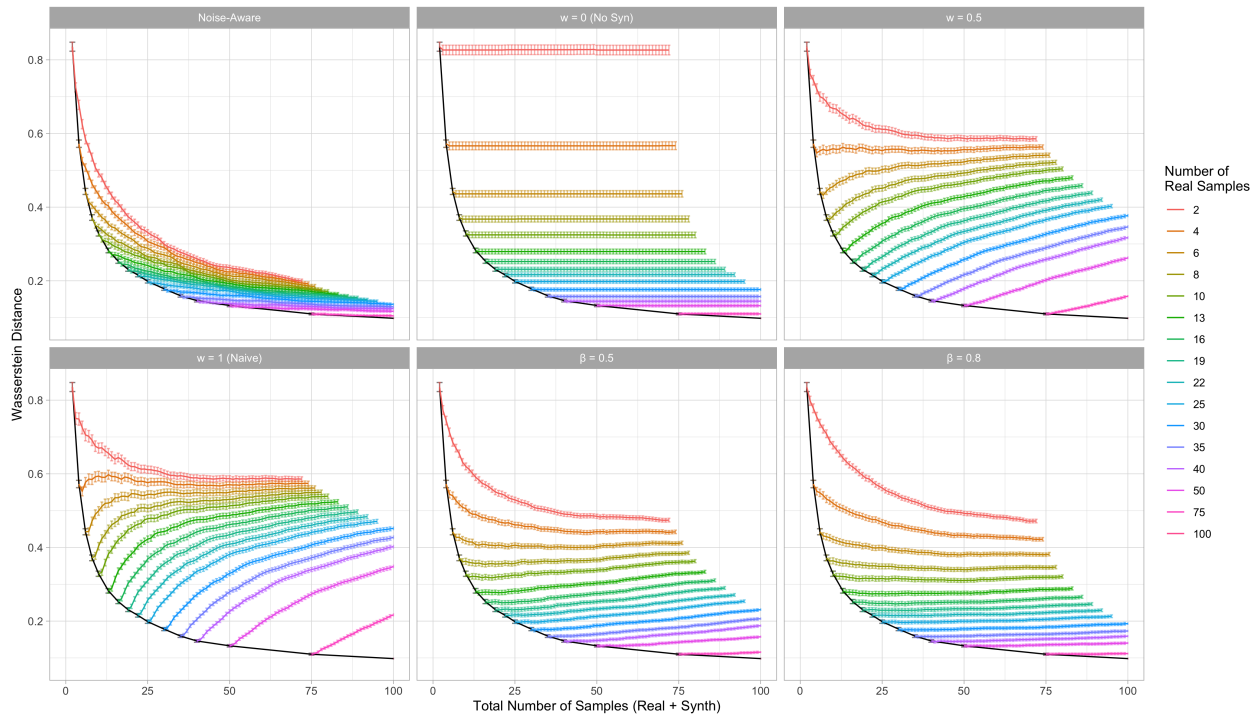


Figure A.11: Branching plots for each model configuration in the case of the simulated Gaussian experiments illustrating the Wasserstein distance against the total number of samples where DP of $\epsilon = 6$ is achieved by the Laplace mechanism via noise of scale $\lambda = 1.0$.

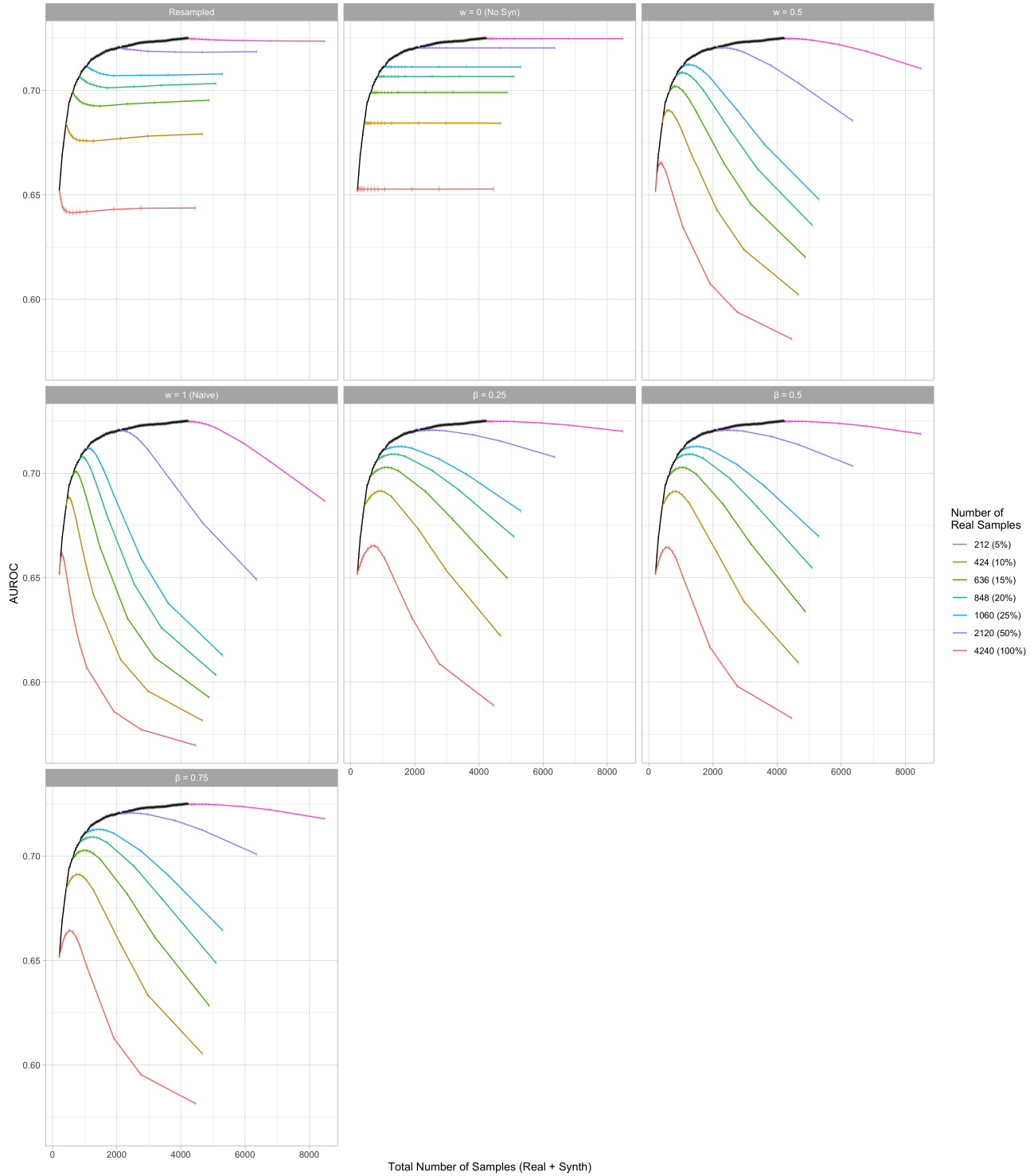


Figure A.12: Branching plots for each model configuration in the case of the logistic regression experiments on the Framingham dataset illustrating the AUROC against the total number of samples where DP of $\epsilon = 6$ is achieved via generation of synthetic datasets using the PATE-GAN.

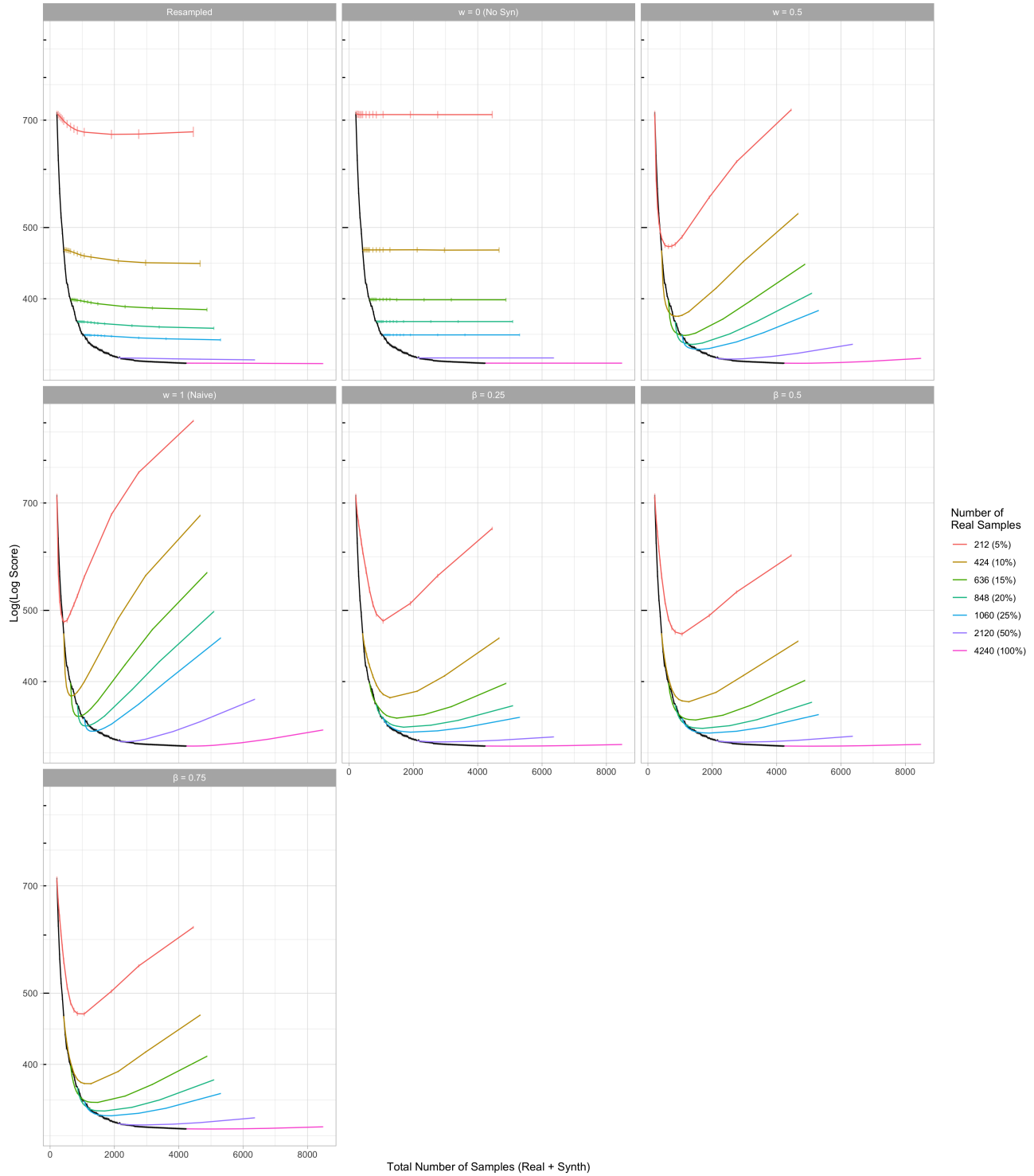


Figure A.13: Branching plots for each model configuration in the case of the logistic regression experiments on the Framingham dataset illustrating the log score against the total number of samples where DP of $\epsilon = 6$ is achieved via generation of synthetic datasets using the PATE-GAN.

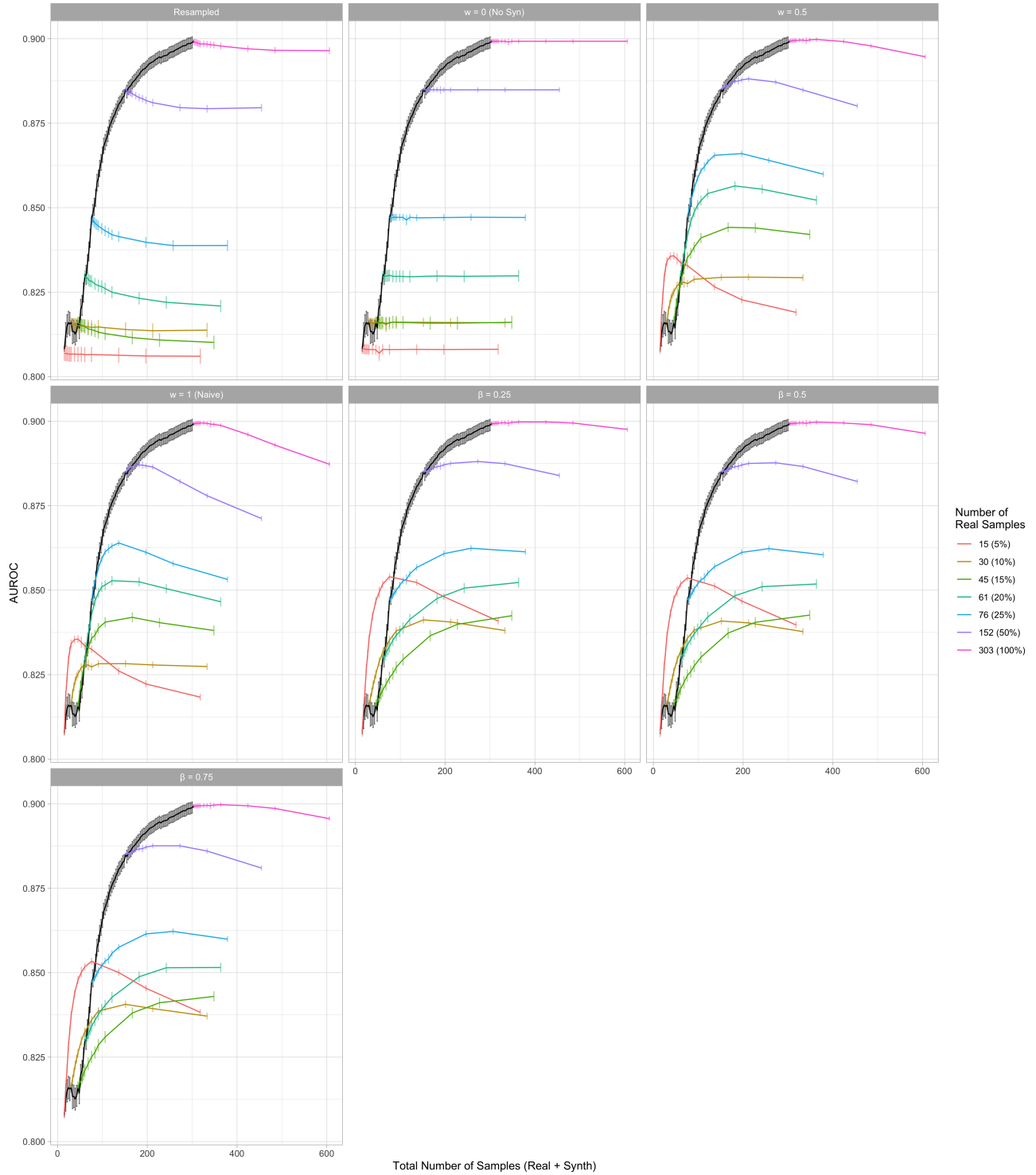


Figure A.14: Branching plots for each model configuration in the case of the logistic regression experiments on the UCI Heart dataset illustrating the AUROC against the total number of samples where DP of $\epsilon = 6$ is achieved via generation of synthetic datasets using the PATE-GAN.

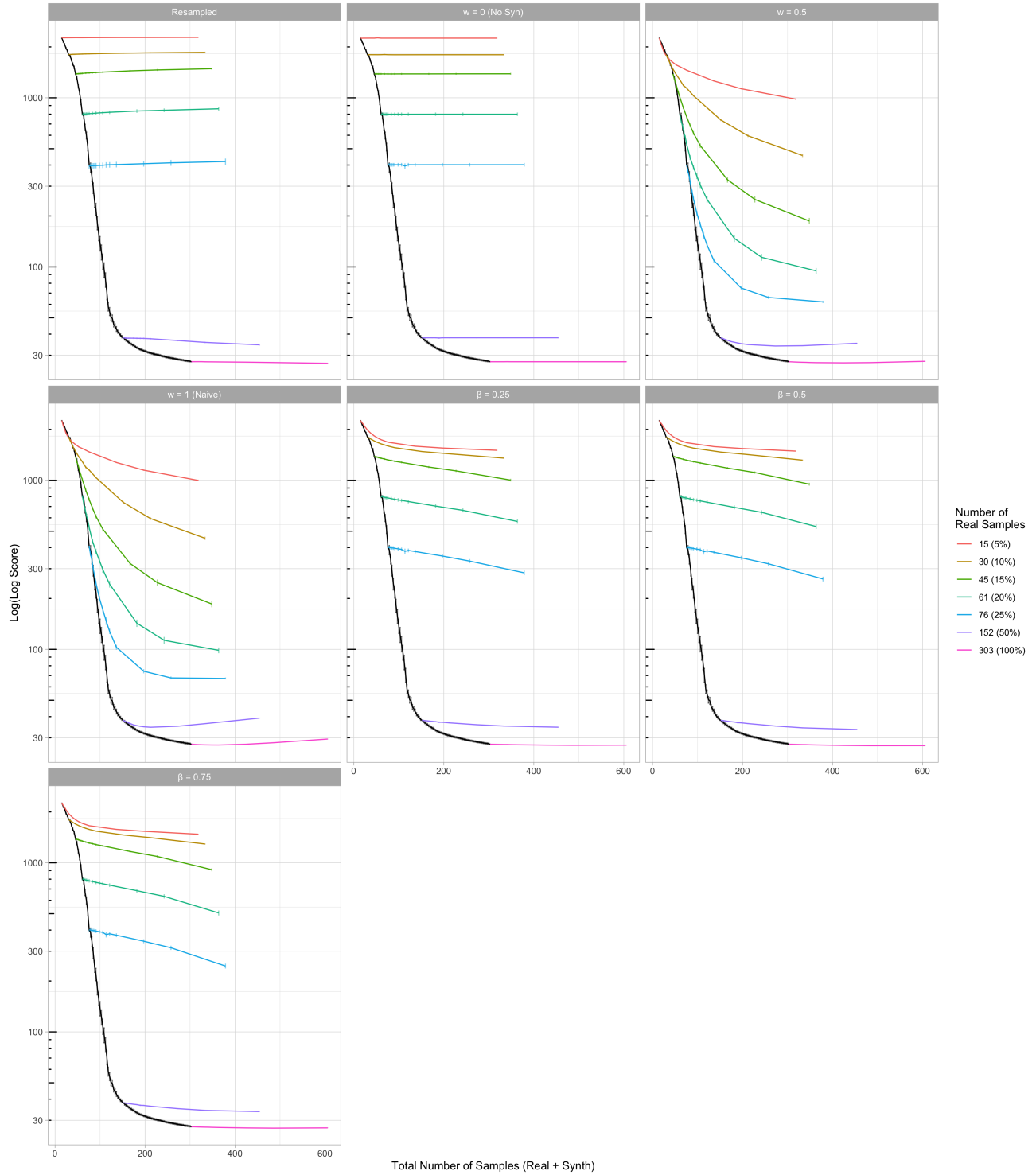


Figure A.15: Branching plots for each model configuration in the case of the logistic regression experiments on the UCI Heart dataset illustrating the log score against the total number of samples where DP of $\varepsilon = 6$ is achieved via generation of synthetic datasets using the PATE-GAN.

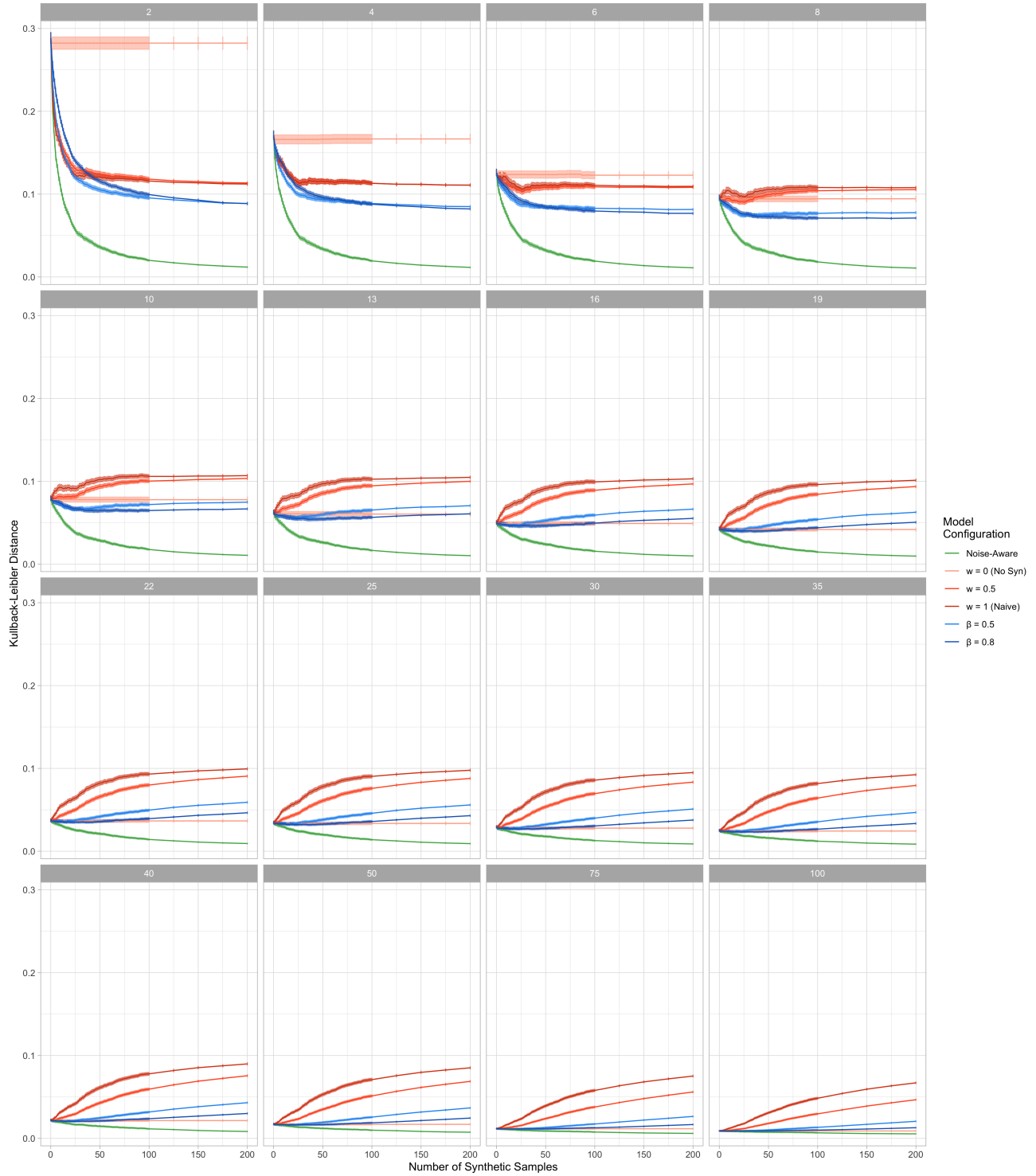


Figure A.16: Model comparison plots for each real data quantity n_L in the case of the simulated Gaussian experiments illustrating the KLD against the number of synthetic samples where DP of $\epsilon = 8$ is achieved by the Laplace mechanism via noise of scale $\lambda = 0.75$.

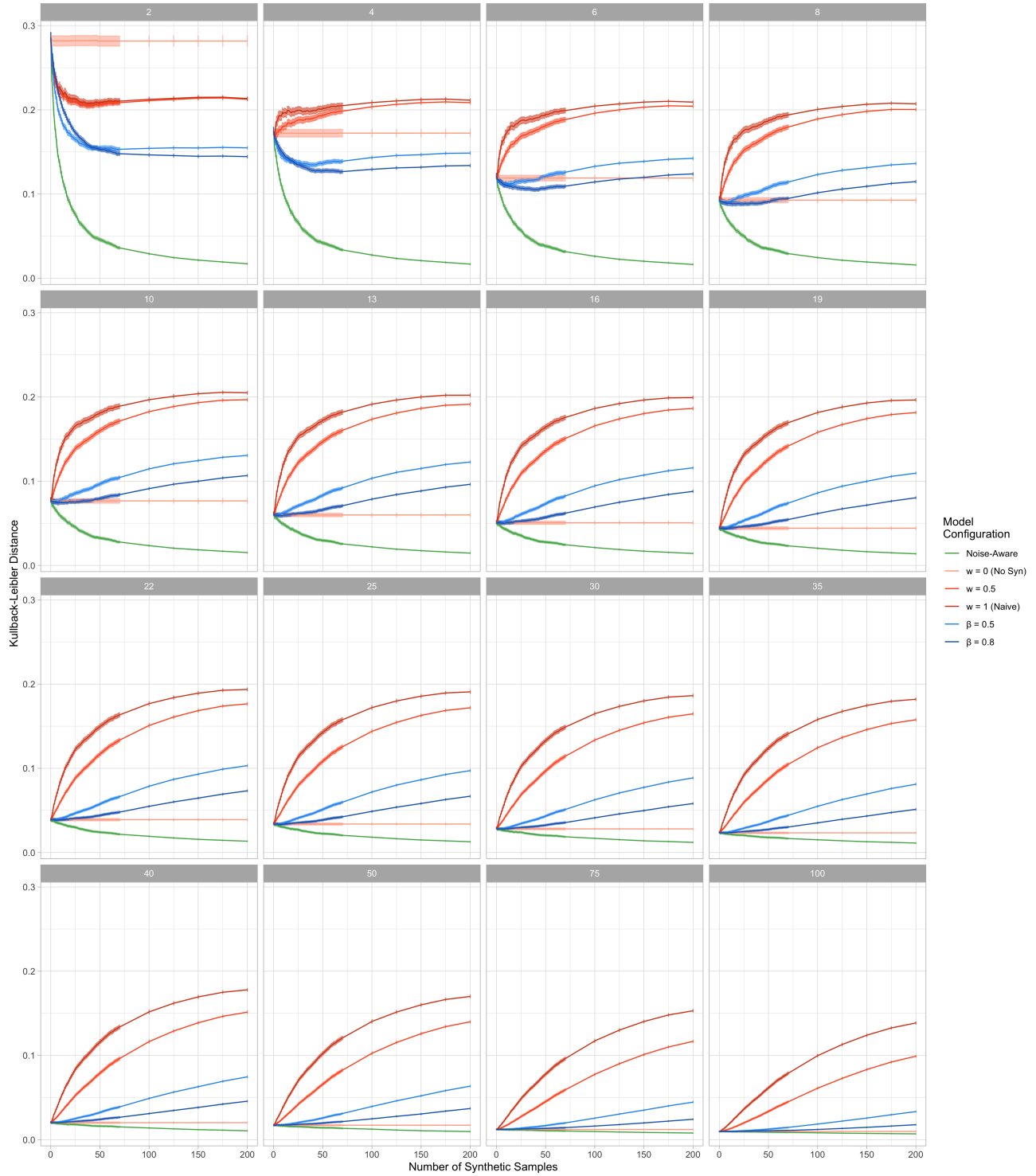


Figure A.17: Model comparison plots for each real data quantity n_L in the case of the simulated Gaussian experiments illustrating the KLD against the number of synthetic samples where DP of $\epsilon = 6$ is achieved by the Laplace mechanism via noise of scale $\lambda = 1.0$.

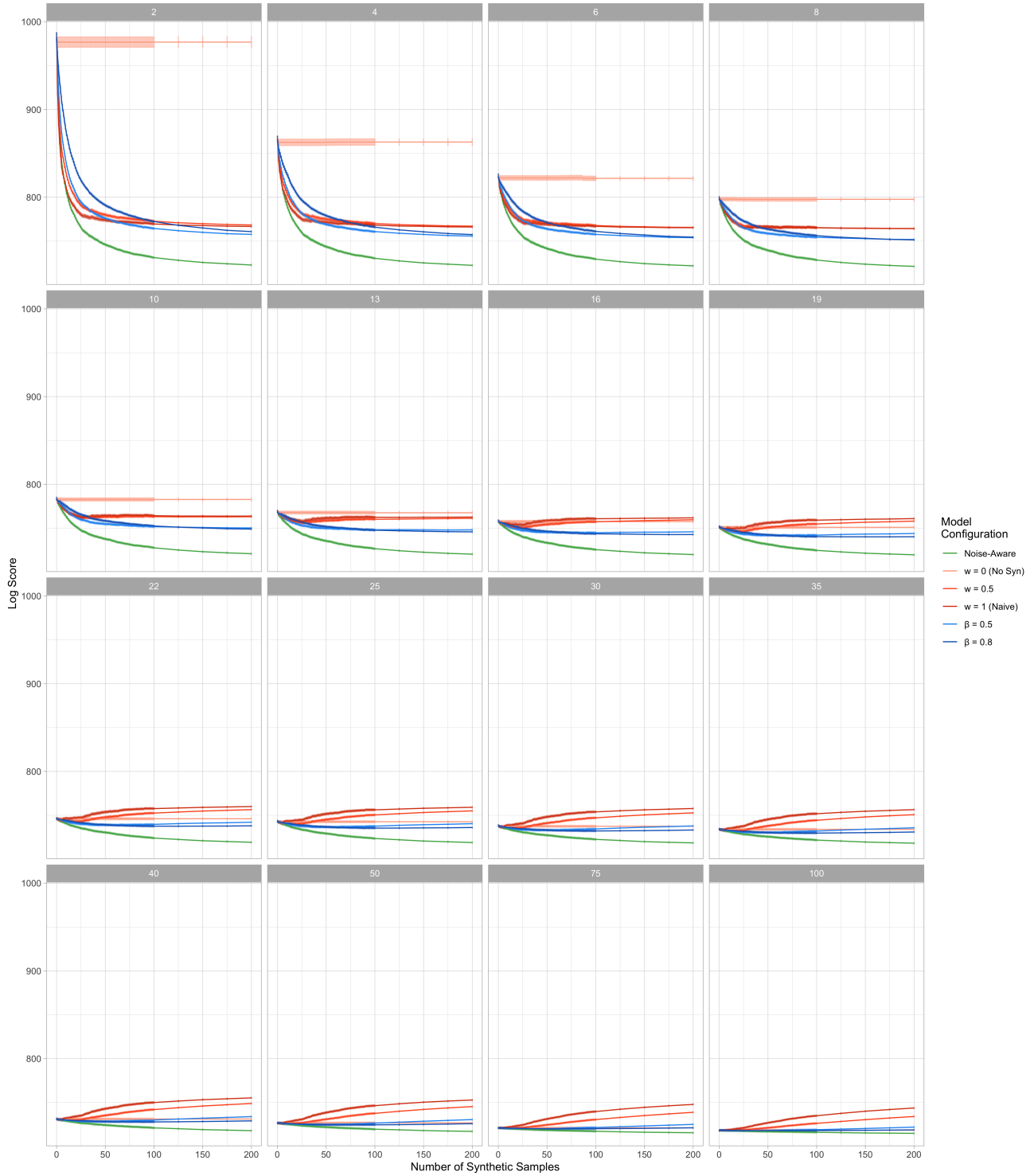


Figure A.18: Model comparison plots for each real data quantity n_L in the case of the simulated Gaussian experiments illustrating the log score against the number of synthetic samples where DP of $\varepsilon = 8$ is achieved by the Laplace mechanism via noise of scale $\lambda = 0.75$.

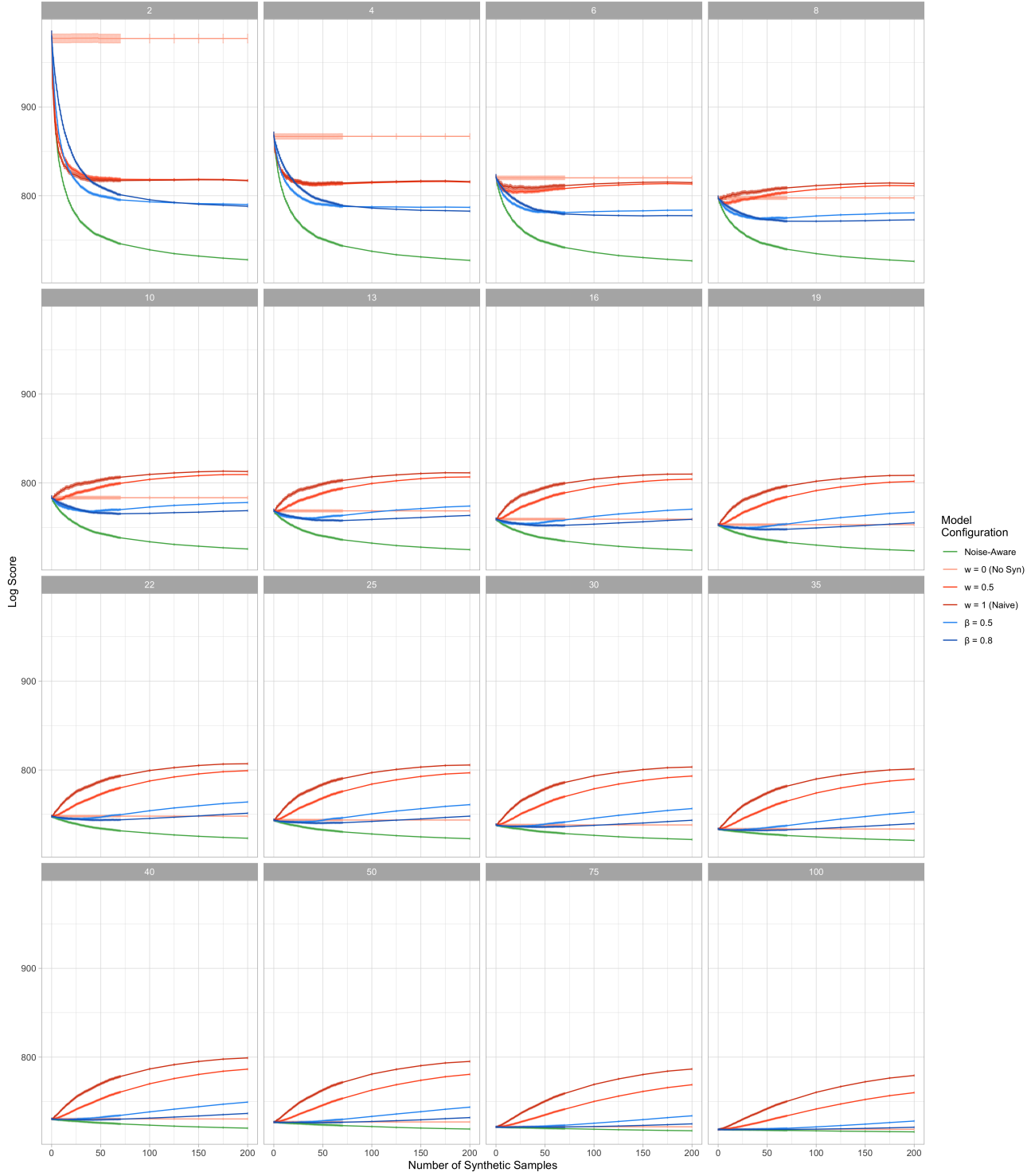


Figure A.19: Model comparison plots for each real data quantity n_L in the case of the simulated Gaussian experiments illustrating the log score against the number of synthetic samples where DP of $\varepsilon = 6$ is achieved by the Laplace mechanism via noise of scale $\lambda = 1.0$.

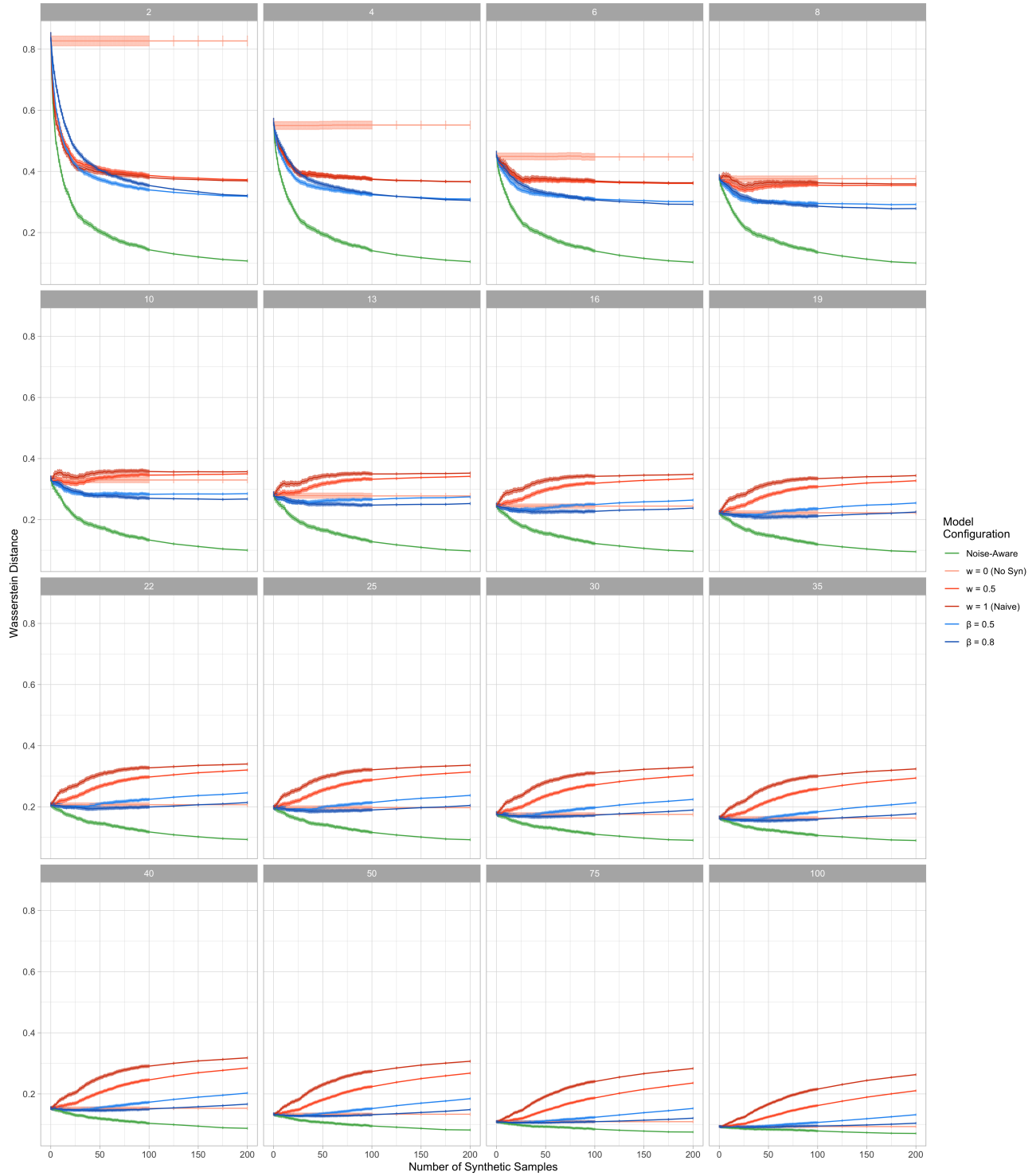


Figure A.20: Model comparison plots for each real data quantity n_L in the case of the simulated Gaussian experiments illustrating the Wasserstein distance against the number of synthetic samples where DP of $\epsilon = 8$ is achieved by the Laplace mechanism via noise of scale $\lambda = 0.75$.

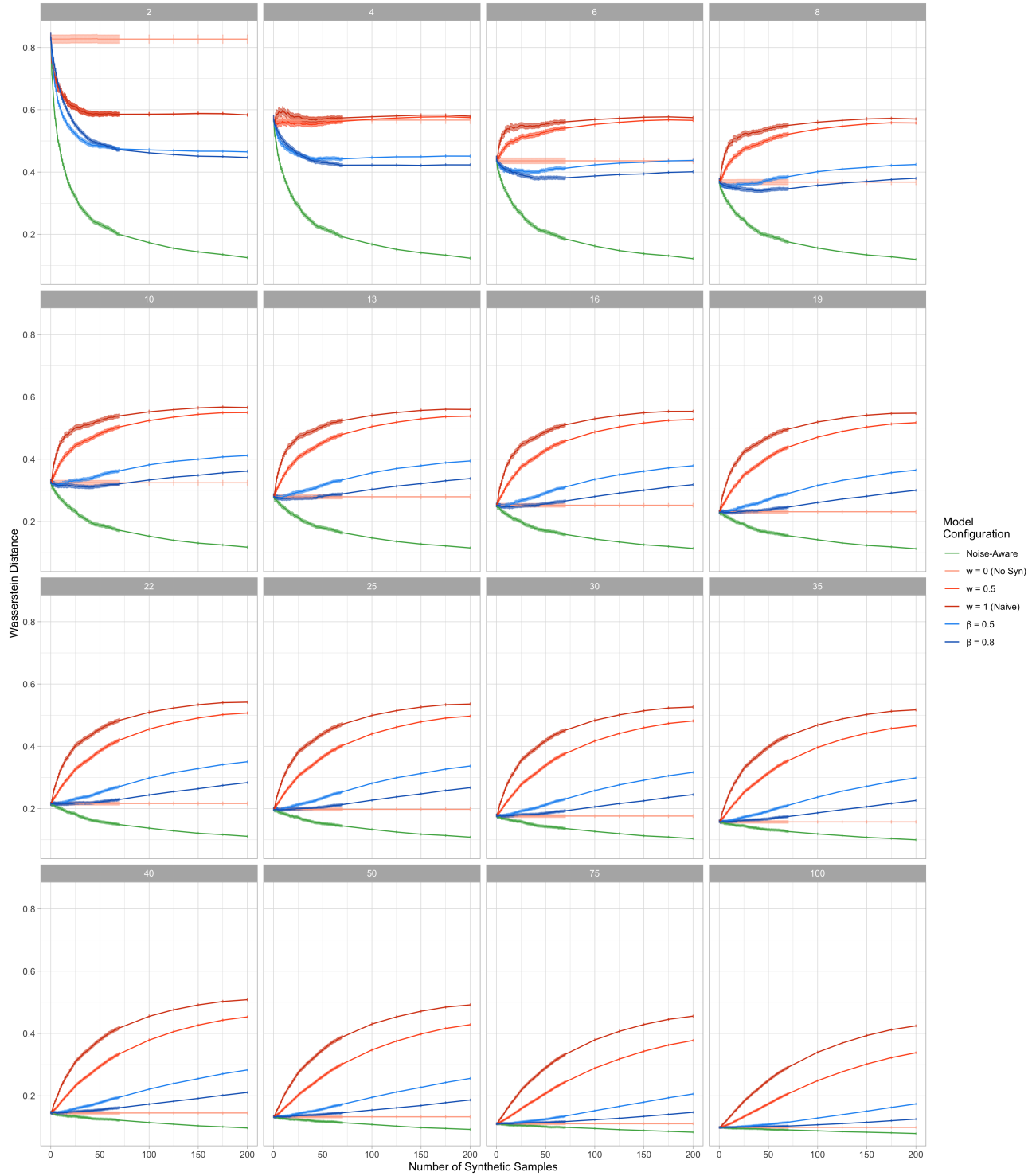


Figure A.21: Model comparison plots for each real data quantity n_L in the case of the simulated Gaussian experiments illustrating the Wasserstein distance against the number of synthetic samples where DP of $\epsilon = 6$ is achieved by the Laplace mechanism via noise of scale $\lambda = 1.0$.

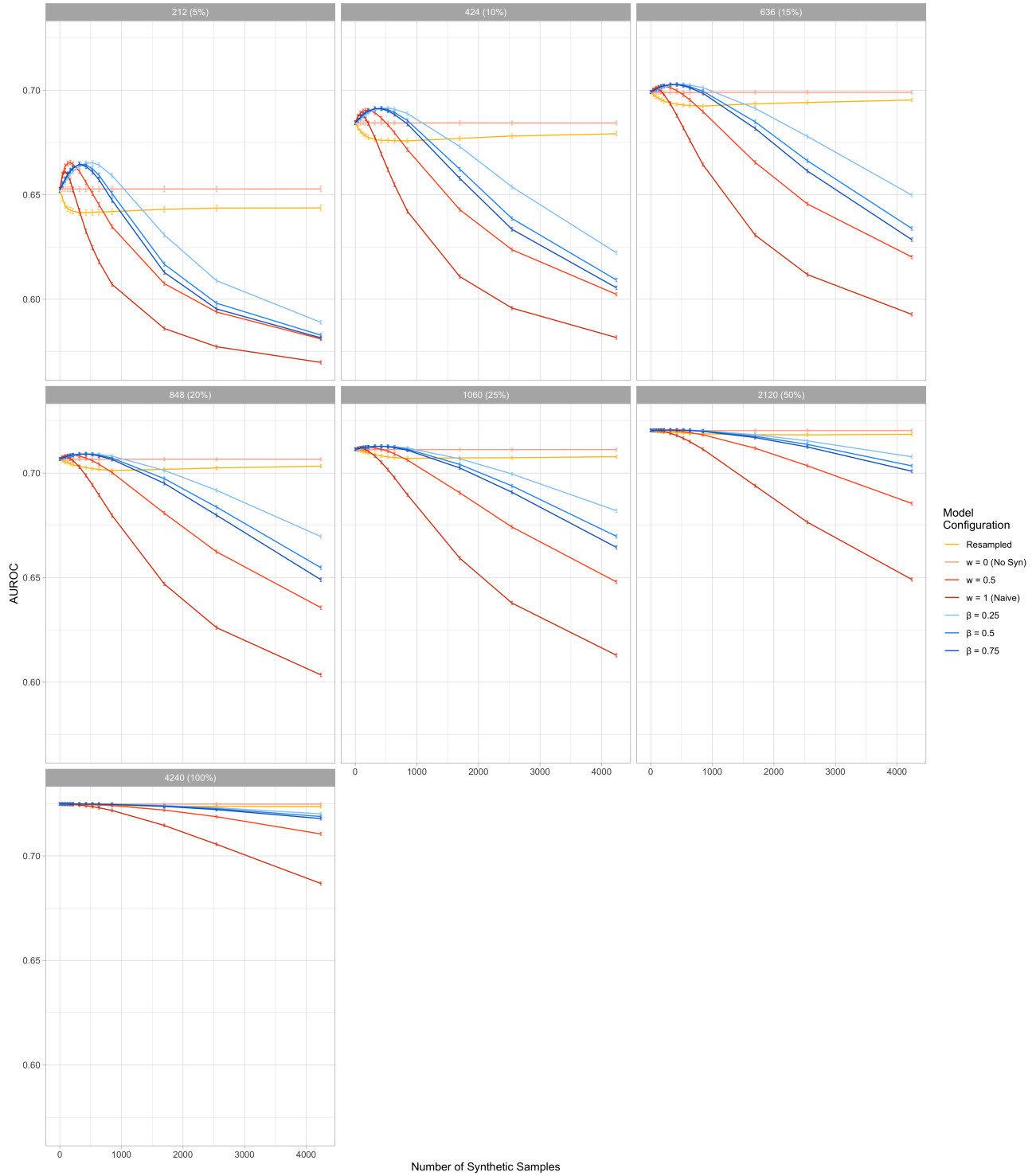


Figure A.22: Model comparison plots for each real data quantity n_L in the case of the logistic regression experiments on the Framingham dataset illustrating the AUROC against the number of synthetic samples where DP of $\epsilon = 6$ is achieved via generation of synthetic datasets using the PATE-GAN.

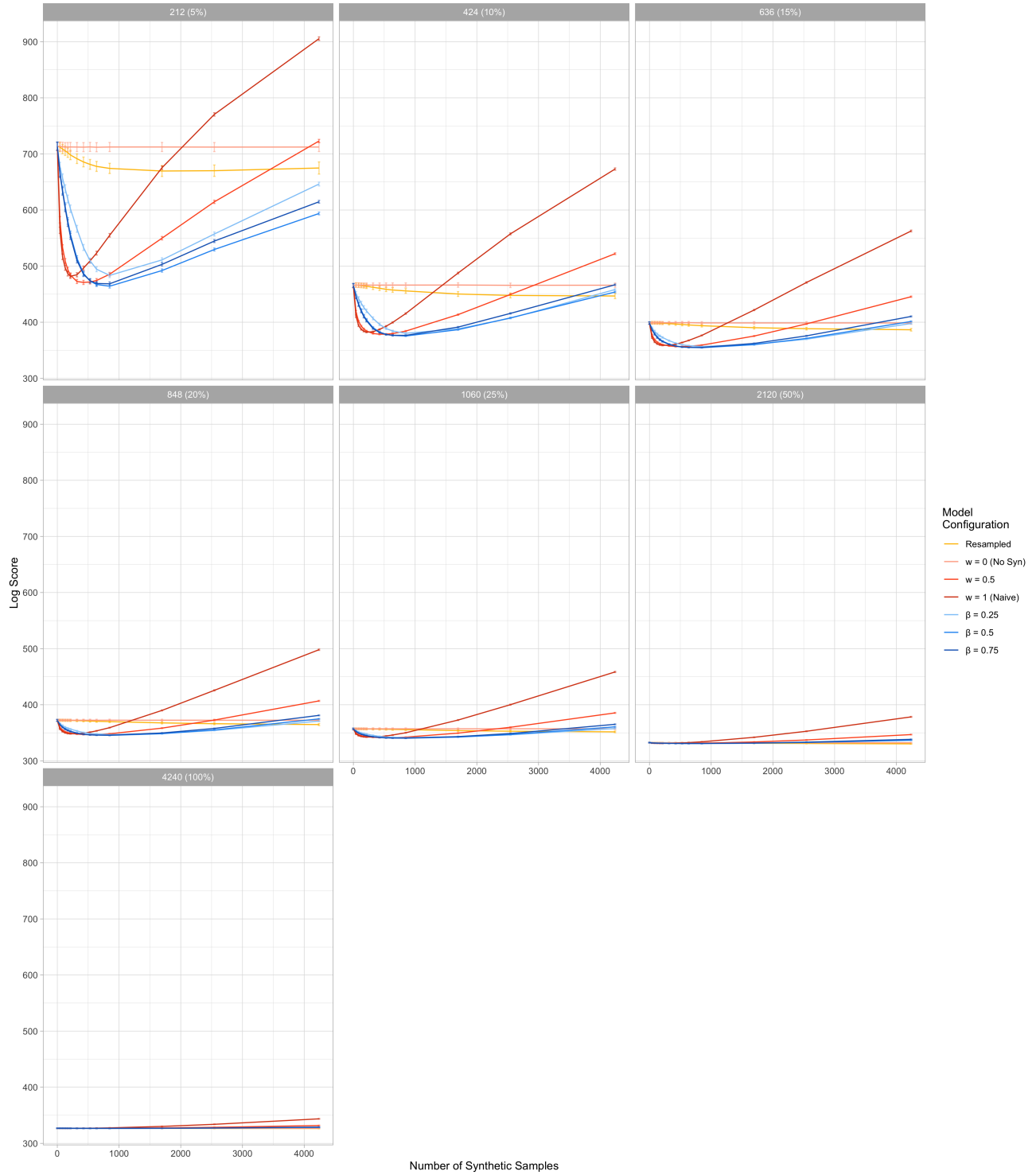


Figure A.23: Model comparison plots for each real data quantity n_L in the case of the logistic regression experiments on the Framingham dataset illustrating the AUROC against the number of synthetic samples where DP of $\epsilon = 6$ is achieved via generation of synthetic datasets using the PATE-GAN.

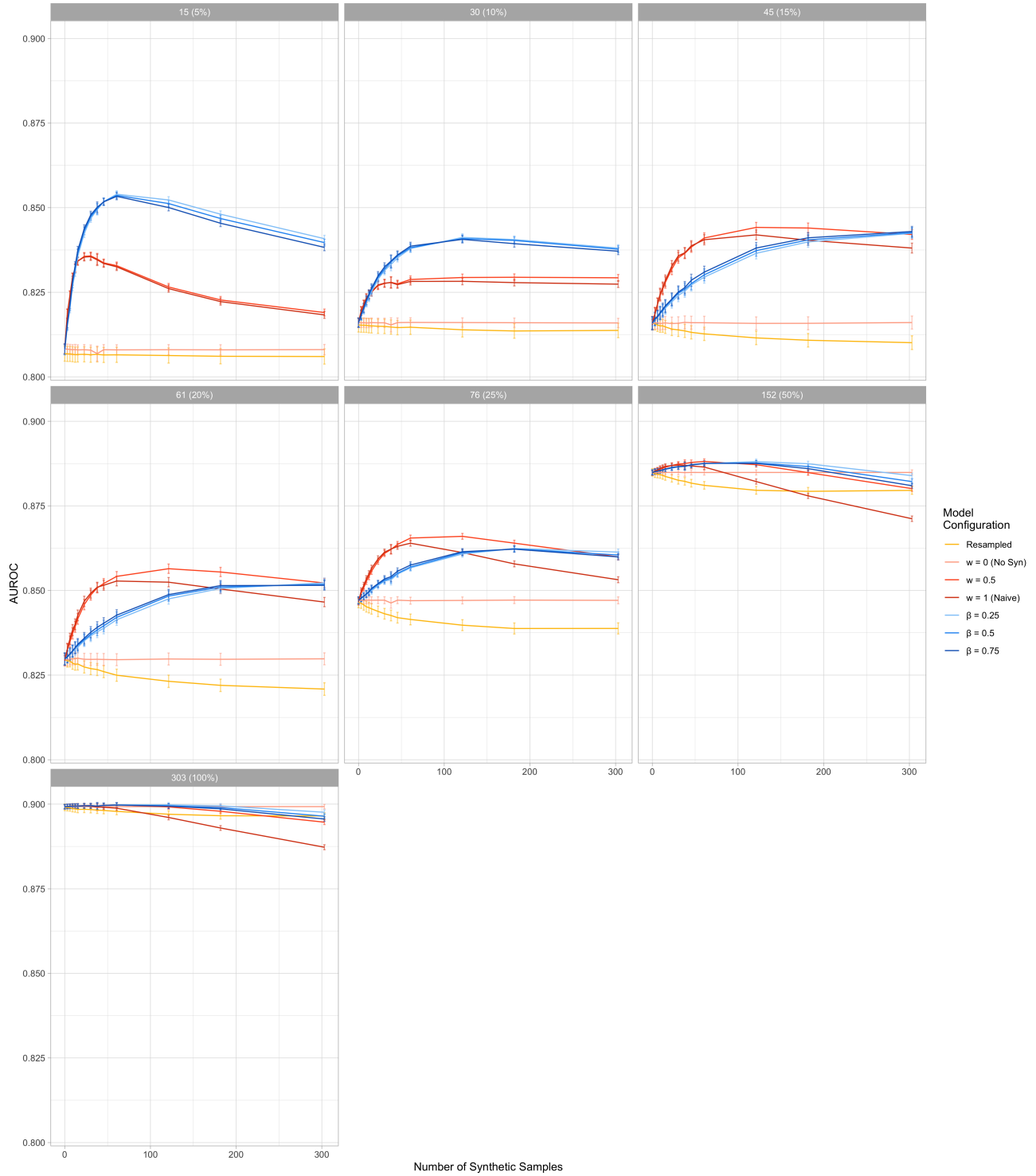


Figure A.24: Model comparison plots for each real data quantity n_L in the case of the logistic regression experiments on the UCI Heart dataset illustrating the AUROC against the number of synthetic samples where DP of $\epsilon = 6$ is achieved via generation of synthetic datasets using the PATE-GAN.

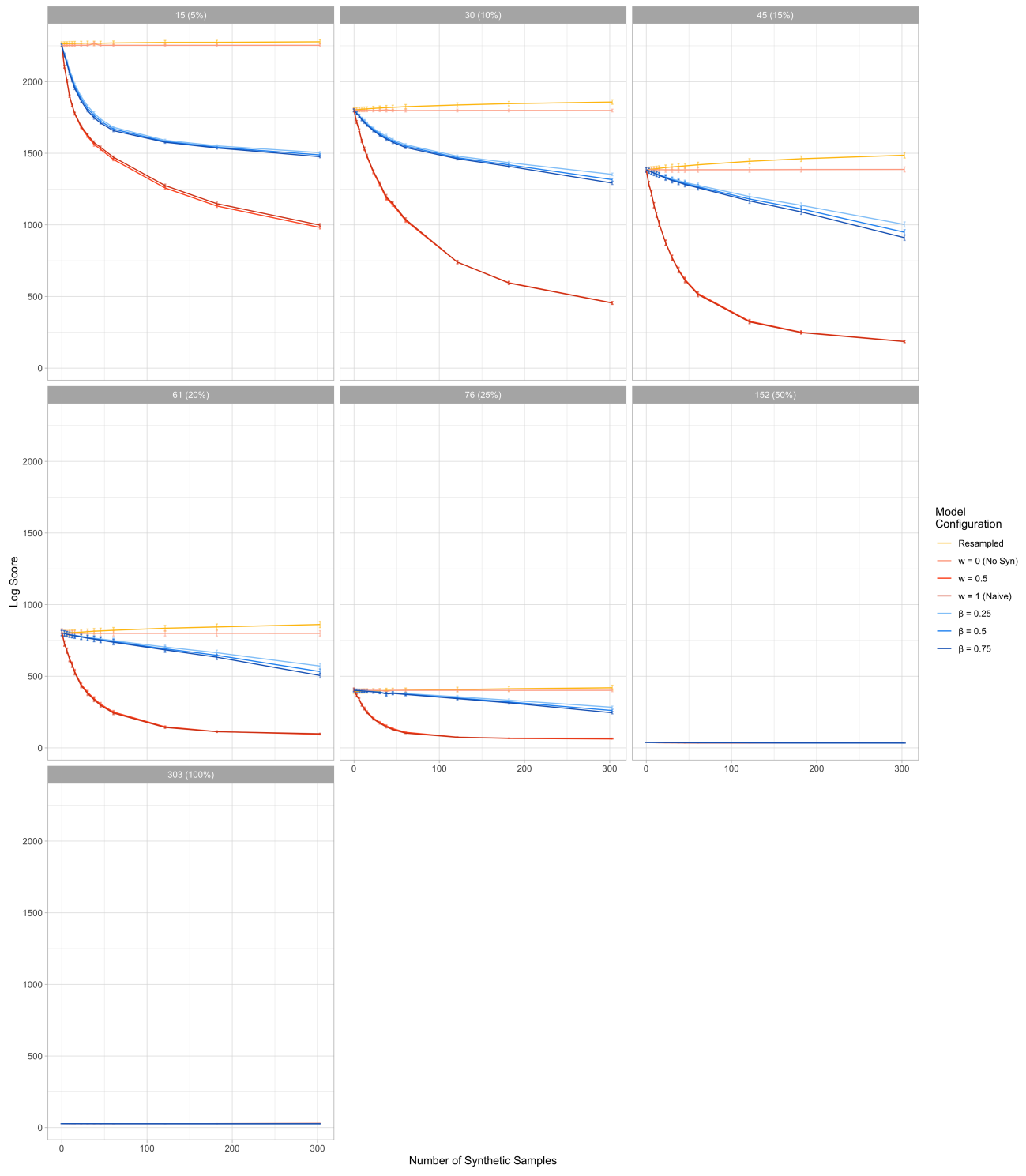


Figure A.25: Model comparison plots for each real data quantity n_L in the case of the logistic regression experiments on the UCI Heart dataset illustrating the AUROC against the number of synthetic samples where DP of $\epsilon = 6$ is achieved via generation of synthetic datasets using the PATE-GAN.

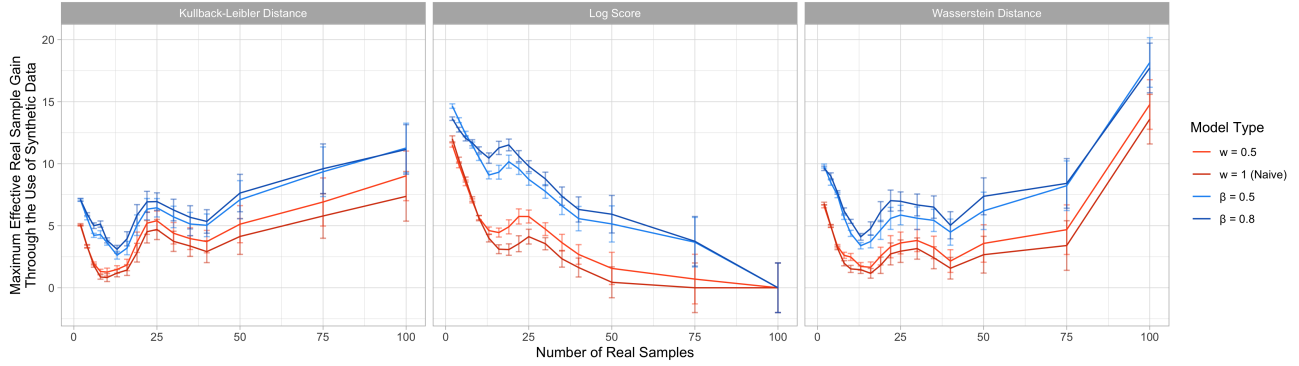


Figure A.26: n -effective plots for each of the relevant criteria in the case of the simulated Gaussian experiments illustrating the effective number of real samples to be gained through the use of synthetic data at each amount of real data n_L where DP of $\varepsilon = 8$ is achieved by the Laplace mechanism via noise of scale $\lambda = 0.75$.

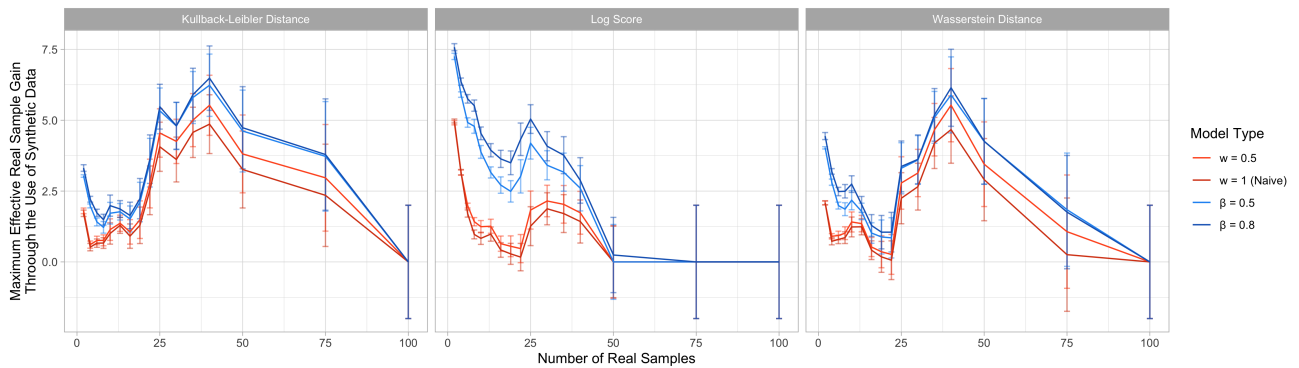


Figure A.27: n -effective plots for each of the relevant criteria in the case of the simulated Gaussian experiments illustrating the effective number of real samples to be gained through the use of synthetic data at each amount of real data n_L where DP of $\varepsilon = 6$ is achieved by the Laplace mechanism via noise of scale $\lambda = 1.0$.

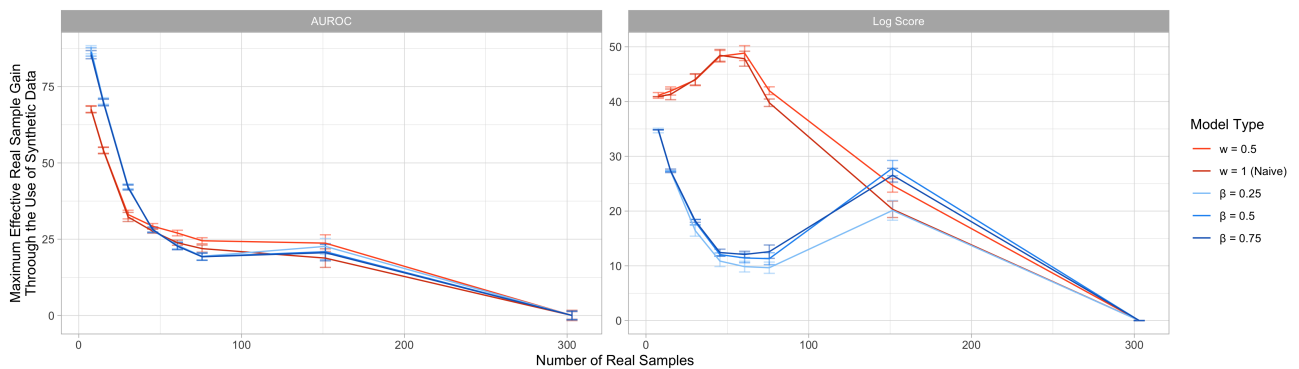


Figure A.28: n -effective plots for each of the relevant criteria in the case of the logistic regression experiments on the UCI Heart dataset illustrating the effective number of real samples to be gained through the use of synthetic data at each amount of real data n_L where DP of $\varepsilon = 6$ is achieved via generation of synthetic datasets using the PATE-GAN.

References

- Amini, Z. and Rabbani, H. (2017). Letter to the editor: Correction to “the normal-laplace distribution and its relatives”. *Communications in Statistics-Theory and Methods*, 46(4):2076–2078.
- Basu, A., Harris, I. R., Hjort, N. L., and Jones, M. (1998). Robust and efficient estimation by minimising a density power divergence. *Biometrika*, 85(3):549–559.
- Berk, R. H. et al. (1966). Limiting behavior of posterior distributions when the model is incorrect. *The Annals of Mathematical Statistics*, 37(1):51–58.
- Bernstein, G. and Sheldon, D. R. (2018). Differentially private bayesian inference for exponential families. In *Advances in Neural Information Processing Systems*, pages 2919–2929.
- Bissiri, P., Holmes, C., and Walker, S. G. (2016). A general framework for updating belief distributions. *Journal of the Royal Statistical Society: Series B (Statistical Methodology)*.
- Blaom, A. D., Kiraly, F., Lienart, T., Simillides, Y., Arenas, D., and Vollmer, S. J. (2020). MLJ: A Julia package for composable Machine Learning.
- Calders, T. and Jaroszewicz, S. (2007). Efficient AUC optimization for classification. In *Knowledge Discovery in Databases: PKDD 2007*, pages 42–53. Springer Berlin Heidelberg.
- Carpenter, B., Gelman, A., Hoffman, M. D., Lee, D., Goodrich, B., Betancourt, M., Brubaker, M., Guo, J., Li, P., and Riddell, A. (2017). Stan: A probabilistic programming language. *Journal of statistical software*, 76(1).
- Dwork, C., McSherry, F., Nissim, K., and Smith, A. (2006). Calibrating noise to sensitivity in private data analysis. In *Theory of cryptography conference*, pages 265–284. Springer.
- Dwork, C., Roth, A., et al. (2014). The algorithmic foundations of differential privacy. *Foundations and Trends in Theoretical Computer Science*, 9(3-4):211–407.
- Efron, B. and Tibshirani, R. J. (1994). *An introduction to the bootstrap*. CRC press.
- Ge, H., Xu, K., and Ghahramani, Z. (2018). Turing: a language for flexible probabilistic inference. In *International Conference on Artificial Intelligence and Statistics, AISTATS 2018, 9-11 April 2018, Playa Blanca, Lanzarote, Canary Islands, Spain*, pages 1682–1690.
- Ghosh, A. and Basu, A. (2016). Robust bayes estimation using the density power divergence. *Annals of the Institute of Statistical Mathematics*, 68(2):413–437.
- Gneiting, T. and Raftery, A. E. (2007). Strictly proper scoring rules, prediction, and estimation. *Journal of the American Statistical Association*, 102(477):359–378.
- Hoffman, M. D. and Gelman, A. (2014). The no-u-turn sampler: adaptively setting path lengths in hamiltonian monte carlo. *J. Mach. Learn. Res.*, 15(1):1593–1623.
- Jewson, J., Smith, J., and Holmes, C. (2018). Principles of Bayesian inference using general divergence criteria. *Entropy*, 20(6):442.
- Jordon, J., Yoon, J., and van der Schaar, M. (2018). Pate-gan: Generating synthetic data with differential privacy guarantees. In *International Conference on Learning Representations*.
- Kurtek, S. and Bharath, K. (2015). Bayesian sensitivity analysis with the fisher-rao metric. *Biometrika*, 102(3):601–616.
- Meinshausen, N., Meier, L., and Bühlmann, P. (2009). P-values for high-dimensional regression. *Journal of the American Statistical Association*, 104(488):1671–1681.
- Reed, W. J. (2006). The normal-laplace distribution and its relatives. In *Advances in distribution theory, order statistics, and inference*, pages 61–74. Springer.
- Rueshendorff, L. (1977). Wasserstein metric. http://encyclopediaofmath.org/index.php?title=Wasserstein_metric&oldid=50083. Accessed: 2020-10-22.
- Watson, J. A. and Holmes, C. C. (2020). Machine learning analysis plans for randomised controlled trials: detecting treatment effect heterogeneity with strict control of type i error. *Trials*, 21(1):156.
- Xie, L., Lin, K., Wang, S., Wang, F., and Zhou, J. (2018). Differentially private generative adversarial network. *arXiv preprint arXiv:1802.06739*.